THE SCIURIDAE (RODENTIA: MAMMALIA) OF CAVE BASIN (OREGON), A NEW MIDDLE MIOCENE MICROFOSSIL LOCALITY

by

EVA MARIE BIEDRON

A THESIS

Presented to the Department of Geological Sciences
and the Robert D. Clark Honors College
in partial fulfillment of the requirements for the degree of
Bachelor of Science

July 2016

An Abstract of the Thesis of

Eva Marie Biedron for the degree of Bachelor of Sciences
in the Department of Geological Sciences to be taken July 2016

Title: The Sciuridae (Rodentia: Mammalia) of Cave Basin (Oregon), a new Middle Miocene microfossil locality

Approved: ______________________________
Dr. Samantha S. B. Hopkins

Cave Basin is a Mid-Miocene vertebrate fossil site located on the South Fork of the Crooked River, near Paulina in Central Oregon. In this basin, the Mascall Formation is composed of tuffs, paleosols, diatomites, fluvial and lacustrine sediments, producing floral, macrofaunal, and microfaunal vertebrate fossils. I describe seven genera of squirrels from the Cave Basin fauna, including a new latest Hemingfordian boundary species of *Miospermophilus* and the first record of *Miopetaurista* in the Miocene of North America. The sediments and diverse community of terrestrial, arboreal, and semi-fossorial squirrels found at Cave Basin indicate an environment supporting woodland, marginal forest, and non-forest environments around a body/bodies of water with non-permanent boundaries. The Cave Basin assemblage provides a window into the diversity of local environments and mammalian communities present during the Mid-Miocene Climatic Optimum. Additionally, the Cave Basin sciurid assemblage is one of the most diverse in Oregon and highlights the range of micromammal niches available in mixed environments.

Acknowledgements

I would like to thank my committee: Dr. Samantha Hopkins for her help in developing this project and her guidance during the completion of this work, Dr. Edward Davis for his advice on paleoecological topics and raptor taphonomy, and Win McLaughlin for her support and for sharing her knowledge of (and enthusiasm for) squirrels.

This project could not have been completed without the hard work of Dr. David Whistler, who prepared the specimens, Dr. Ray Weldon, who taught me about the geology of the Cave Basin site, and Nicholas Famoso, who guided me in the curation of these specimens. Thank you all.

Thanks to the wonderful communities at the University of Oregon Vertebrate Paleontology Lab and the Museum of Natural and Cultural History, my wonderful family and friends, and to anyone who’s ever listened to me make an awful squirrel-themed joke (and made one back). Thanks for supporting me through three nutty years!

Table of Contents

List of Figures

List of Tables

INTRODUCTION

The Middle Miocene Mascall Formation of the John Day region (in Central and Western Oregon) has long held the interest of paleontologists studying Miocene mammals and ecosystems. Mascall sediments are also exposed in the Crooked River Basin (South-Central Oregon), but this region has not been systematically collected since the middle of the twentieth century. The Crooked River Basin has a collection record stretching at least to the early 1880s and has been prospected and/or discussed by Cope, Merriam, Davis, Day, and Marsh (Downs, 1956). However, these investigations do not appear to include any outcrops south of Paulina, Oregon. Investigations within the last five years by the University of Oregon Vertebrate Paleontology Lab have identified two regions of interest: Hawk Rim (McLaughlin *et al.*, 2016) and Cave Basin, the topic of this work.

The South Fork of the Crooked River runs through a valley whose steep-sided slopes expose parts of the John Day Formation, Columbia River Basalts, Mascall Formation, and Rattlesnake Formation (or their equivalent). Several tuffs yield radiometric dates, including the Hawk Rim Tuff (HRT) and the Rattlesnake Ash Flow Tuff (RAFT). In the Crooked River Mascall, the HRT dates to the latest Hemingfordian (16.260 ± 0.009 MA via ^{206}Pb/^{238}U dating, McLaughlin *et al.*, 2016) and underlies the sediments of Cave Basin. The RAFT (7.05 ± 0.1 MA via ^{40}Ar/^{39}Ar dating, Streck, 1995) marks the upper boundary of the Mascall Formation and is the first stratigraphic unit of the Rattlesnake Formation. Biostratigraphically significant fossils such as *Pseudaelurus skinneri*, *Moropus*, and *Rakomeryx* indicate the Hawk Rim Mascall Formation is late

Hemingfordian. Given that Cave Basin site is only slightly stratigraphically higher than the Hawk Rim site, the Cave Basin field site is likely latest Hemingfordian as well.

Paleontologists have studied the lower Mascall Formation sediments of the John Day Basin for their rich floral, faunal, and environmental record of the Mid-Miocene Climatic Optimum (MMCO). The warm, wet, and well-forested MMCO differed from earlier shrub-land and later sod grassland landscapes (Retallack, 2009). The abundance of macrofloral fossils (such as leaves) indicates the area covered by the Mascall Formation was heavily vegetated. Swamp cypresses, Dawn Redwood, oaks, maples, elms, hickories, and birches are common members of Mascall forests, but grass macrofossils are not reported (Dilloff, 2009). Chaney (1925, 1956) compared the vegetation to modern cold-winter deciduous forests, but more recent reconstructions describe a hardwood-dominated forest with swampy regions dominated by cypress trees (Dillhoff, 2009). Several genera of algae (*Tetraedron sp.*, *Botryococcus sp.*, and *Pediastrum sp.*) have been found in the John Day Basin Mascall, apparently from the lower fossil flora producing portions, supporting sediment interpretations of wet environments (Gray, 1960). Of these algae, *Pediastrum* is a benthic freshwater alga, while both *Botryococcus* and *Tetraedron* are able to survive in both freshwater and brackish environments, perhaps like ponds in the cypress swamps.

Phyotolith data provides a more nuanced view of the Mascall flora, both confirming wetland environments and suggesting the presence of drier grassy regions. Palm, ginger, and aquatic-type phytoliths were found, reinforcing the interpretation of a warm, humid climate supporting some wetland and dominant forest environments (Stromberg, 2014). Although rare, the presence of bamboos and pooids (obligate C_3

photosynthesizers) and PACMAD grasses (both C_3 and C_4 photosynthesizers) indicates a diversity of grass-supporting habitats (Stromberg, 2014 and Dunn, 2014). The presence of C_3 grasses supports interpretations of humid forest environments where the canopy would be able to shade these smaller plants. The presence of C_4 grasses denotes comparatively open environments that received frequent sunlight, potentially appearing as forest clearings, meadows, and woodland margins.

The not-entirely-closed environment indicated by floral and phytolith data is also supported by paleopedological data. Paleosols, or fossil soils, are common in the John Day Basin and Crooked River Mascall. Inceptisols, andisols, alfisols, and vertisols are present in John Day Mascall exposures, highlighting the volcanic origin of the Mascall Formation's closed and open environments (Table 1). As the macrofloral data suggests, during their formation, Mascall soils would have supported coniferous Dawn Redwood forests, hardwood forests, and sparsely-forested Cypress swamps. Most of the Mascall soil-types are also known to support shrubby grassland or savannah-like environments, echoing the C_4 phytolith data.

Climate-wise, paleosol and macrofloral data corroborate each other, indicating a generally temperate and humid environment. The duric horizons in many of the Mascall paleosols reported by Bestland (2008) indicate high weathering rates of volcanic ash and other material. In modern systems, humid climates contribute to weathering by preventing soil-water evaporation and allowing for the percolation of silica-containing fluids into lower soil layers. Combining the paleopedological, palynological, macrofloral, and microfloral data indicate the Mascall formation had a humid climate with warm summers and cool to cold winters (Bestland, 2008).

Described Paleosols	Modern analogue	Soil and vegetation characters*
Maqas, Patu, Monana, Yanwa	Inceptisol	Highly variable soils may be very wet near the surface or swamp-like, supporting coniferous forests or shrubby grassland with widely spaced trees
Walask	Andisol	Soil heavy in volcanic alumino-silicates supporting mainly coniferous forests, but sometimes shrubs and grasses
Skwiskwi, Luca	Alfisol	Well-developed, leached soil supporting or has supported coniferous or deciduous forest
Wawcak	Vertisol	Clay-heavy shrink-swell soils supporting open forest or savannah

Paleosols and modern soil analogues drawn from Bestland, 2008
* Environmental interpretations generalized across soil suborders and drawn from *Soil Taxonomy* 2nd Edition (1999) distributed by the USDA.

Table 1. Interpretations of John Day Basin Mascall paleosols

The latest Hemingfordian Hawk Rim field site also yields paleoecological data in the form of faunal fossils. The ungulate fauna of Hawk Rim includes *Merychippus* and *Archeohippus*, corroborating the presence of both forest and marginal forest environments (McLaughlin *et al.*, 2016). Isotopic data indicates *Archeohippus* has a narrow dietary niche, only browsing from crown leaf vegetation of small trees and shrubs in woodland clearings. In contrast, *Merychippus* has an isotopically broad dietary niche suggesting it ate C_3 grasses in both open and closed environments. Additionally, isotope data indicates Oregonian *Merychippus* did not consume C_4 grasses, suggesting C_4 grasses may be rare or absent from the Hawk Rim flora (Maguire, 2015). Hawk Rim is reported to have wet forested environment. The fauna found there corroborate this with the addition that some marginal forest environments, perhaps woodland clearings, may have been present as well.

Cave Basin captures a different environment than the Mascall Formation of the John Day Basin. Comparing the two regions allows for a more complete understanding of broader regional environmental variation during this period. The sediments at Cave Basin site contain a variety of microfossils, including small mammal taxa. Here, I describe the Sciuridae (squirrels) of this assemblage and consider their ecological significance.

There is a strong record of terrestrial and fossorial squirrels in the continental United States, but diversity is often limited to two or three species at each site. The Cave Basin Sciuridae includes three tribes and seven genera. A new species of *Miospermophilus* is described, as well as the complete dentition of a *Protospermophilus* species, previously known only from the John Day Basin Mascall Formation. Multiple genera in both the Tamiini (chipmunk tribe) and Pteromyini (flying squirrel tribe) are present. In conjunction with geological data, I use these Sciuridae to reconstruct the ecology of the Cave Basin site. Understanding the ecology of geographically distinct sites within the same formation can help us reconstruct larger landscapes in terms of habitat heterogeneity and mammalian diversity.

METHODS

The University of Oregon Vertebrate Paleontology lab and University of Oregon Geology Field Camp began collecting in the Crooked River Basin beginning at the Hawk Rim field site in 2010 and expanding to the nearby Cave Basin field site in 2013 (Figure 1). Previously collected micro- and macro- fossils from these sites have been curated at the John Day Fossil Beds National Monument and the Museum of Natural and Cultural History at the University of Oregon. Microfossils were isolated from anthills, weathered sediments, and in-place matrix. The anthill material is composed of Mascall Formation fossils and sediments, Columbia River Basalt-derived volcanic fragments, and recent plant and insect material. Fossil material was concentrated in sediments by dry and wet screening and heavy liquid separation.

Dry screening was performed immediately on some matrix samples to minimize the amount of non-fossil material transported out of the field. Dr. David Whistler screened all previously un-sifted material in Bend, OR with a 0.75 mm mesh to remove silt and clay particles in the matrix. Both the coarse and fine-grained materials were kept separately. Wet screening of loose and in-place matrix was performed in Bend, OR by passing water through layered 2.5 and 0.75 mm screens. If necessary, the in-place matrix was soaked in water overnight to aid in breaking down the sediment before screening. The screen sizes separated coarse material (≥ 2.5 mm) from intermediate sized material (2.5 mm ≥ grain size ≥ 0.7 mm) and fine-grained material (≤ 0.7 mm). The fine-grained material from both dry and wet screening was further screened using a 0.5 mm mesh.

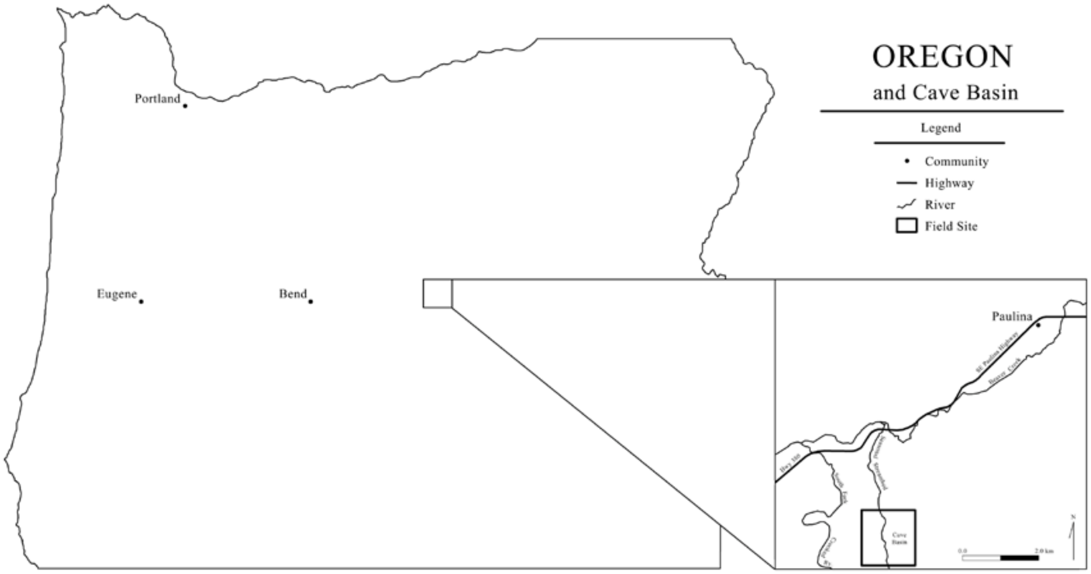

Figure 1. The location of the Cave Basin field site

The Cave Basin field site is located approximately seven miles southeast of Paulina, Oregon. Sediments here are dated to the Late Hemingfordian (Middle Miocene) and from the Mascall Formation.

Heavy liquid separation (HLS) has the ability to preferentially separate fossiliferous material from modern biological and lithic material using the specific gravities of the materials. However, in cases where the specific gravity of lithic materials is close to that of the fossiliferous material, HLS may not be as effective. The sediments of Cave Basin contain basalt fragments which have a specific gravity close to that of fossil enamel and dentine (Basalt: 3.0, Barlow, 1990; Dentine: 2.30, Enamel: 2.9-3.0, McCarty and Congleton, 1994)). Despite this complication, HLS treatment of Cave Basin sediments by Dr. Whistler reduced non-fossiliferous sediments within samples by as much as 75%. HLS was performed using large, custom-made separatory funnels filled with tetrabromoethane (TBE) diluted in acetone. After separation, fossiliferous portions were washed up to 10 times with acetone to remove residual TBE.

These sorting processes enriched the proportion of fossiliferous material in the matrix, making manual matrix picking under magnification easier and more efficient. It also allowed the different size classes of matrix to be sorted under different, fixed levels of magnification, eliminating the likelihood that fossiliferous material was overlooked during a change in magnification. All fossil material was hand-picked to ensure collection of all fossiliferous material including non-identifiable fragments. Fine-grained matrix from the 0.5 mm mesh screens was picked under 20x magnification, while all other size classes were picked under 10x magnification.

The Sciuridae are represented by 293 isolated teeth, of which 167 are identifiable to a genus or species level. Figures 2 and 3 and Table 2 give an explanation of the morphological terms used to describe sciurid dentition. All diagnosable material was pin-mounted using sticky wax or acryloid glue dissolved in acetone and stored in small glass vials. The specimens were photographed using a Dino-Lite Edge electronic microscope (Dinocapture 2.0, ANMO Electronic Corporation). The photographs of the teeth were then digitally measured in ImageJ (Version 1.47, Rasband, 1997-2016). Each specimen was cataloged and curated in the Condon Fossil Collection at the University of Oregon Museum of Natural and Cultural History. Within the Cave Basin site are four locality numbers (UO 4343 Cave Basin, UO 4343 Cave Basin, UO 4343 Cave Basin, and UO 4343 Cave Basin) Specimen photographs and identifications, along with locality information, are available online through the UOMNCH online paleontological catalog at http://paleo.uoregon.edu.

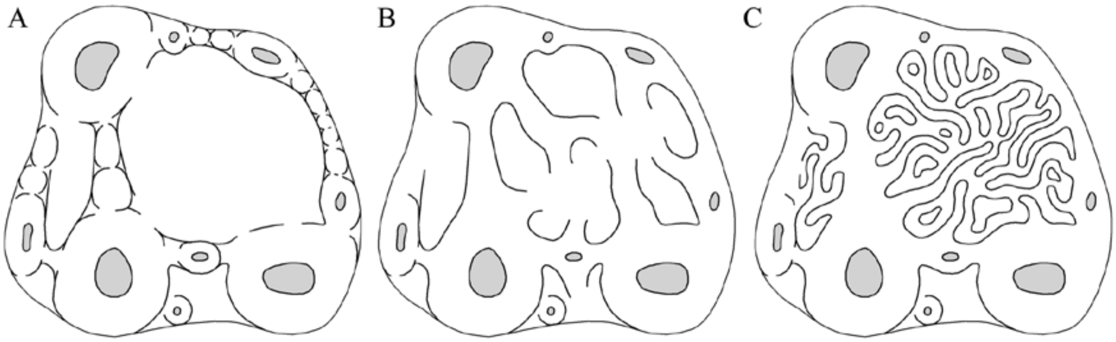

Figure 2. Morphological descriptions of dental rugosity

A. Beaded enamel, B. Lophulate enamel, C. Crenulate enamel. While ‘crenulate’ has been used to describe dental rugosity in Petauristodon (Essenger, 1986), terms describing other enamel complication states were not used. I introduce the terms ‘beaded’ and ‘lophulate’ to fill this gap.

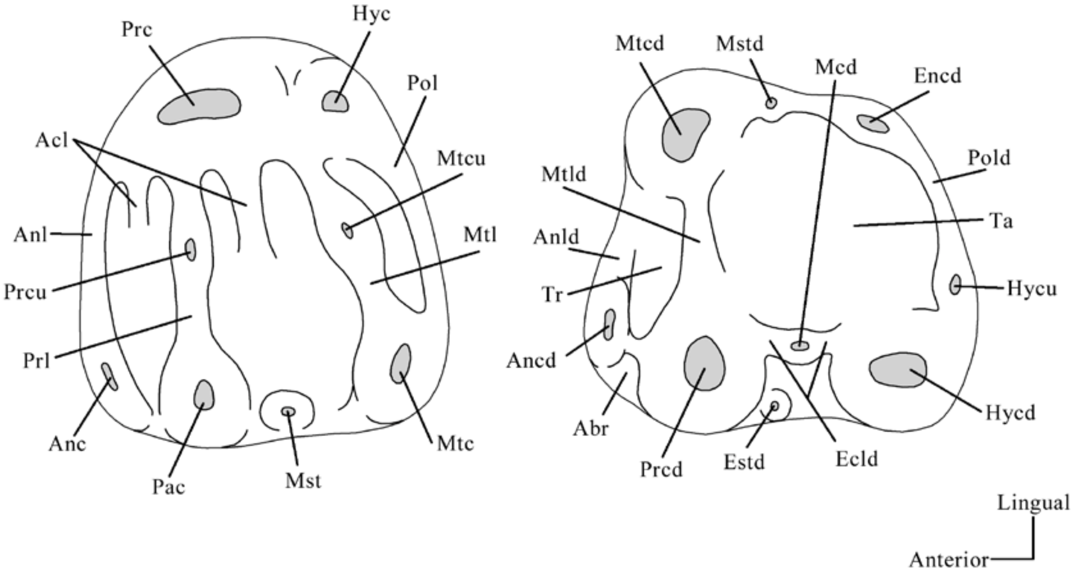

Figure 3. Morphological terms used to describe sciurid dental features

A. Upper molar, B. Lower molar. I generally follow Downs (1956) in regards to terminology. However, I introduce the term ‘anterobuccal re-entrant’ as a replacement for Mein’s (1970) ‘anterosinuside’ and as there was discussion to the validity of the term ‘parastyle’ (pers. comm., Samantha S. B. Hopkins), I adopt Mein’s (1970) terms ‘anteroloph’, ‘anterocone’, ‘anterolophid’, and ‘anteroconid’. Table 2 contains a key for the abbreviated morphological terms.

Upper Dentition		Lower Dentition	
Abbreviation	Term	Abbreviation	Term
Prc	Protocone	Prcd	Protoconid
Hyc	Hypocone	Hycd	Hypoconid
Pac	Paracone	Mtcd	Metaconid
Mtc	Metacone	Encd	Entoconid
Anc	Anterocone	Ancd	Anteroconid
Prcu	Protoconule	Hycu	Hypoconulid
Mtcu	Metaconule	Mcd	Mesoconid
Mst	Mesostyle	Mstd	Mesostylid
Prl	Protoloph	Estd	Ectostylid
Mtl	Metaloph	Mtld	Metalophid
Anl	Anteroloph	Ecld	Ectolophid
Pol	Posteroloph	Anld	Anterolophid
Acl	Accessory lophs*	Pold	Posterolophid
		Tr	Trigonid basin
		Ta	Talonid basin
		Abr	Anterobuccal re-entrant**

* Found only on *Petauristodon*
** Found only on *Miopetaurista*

Table 2. Key to abbreviated morphological terms

Figure 3 diagrams the position of the features on upper and lower teeth.

GEOLOGIC CONTEXT

Cave Basin is located in central Oregon, approximately seven miles from the community of Paulina in Crook County, OR. The Cave Basin sediments represent the Mascall Formation or their equivalent and are characterized by fine-grained deposits of diatomite, clay-rich paleosols, and tuffs. Cave Basin sediments were likely deposited very quickly, with some estimates suggesting a minimum depositional period of half a million years (McLaughlin *et al.*, 2016 and pers. comm., Ray Weldon). The fossiliferous horizons of the Cave Basin site are stratigraphically located no more than 10 meters above the HRT. The short depositional period, rapid sedimentation rates, and proximity to the HRT suggest a possible depositional period occurring from 16.26 MA to approximately 15.75 MA.

The lithology of the Cave Basin sediments allows for hypotheses about the depositional environment. Distal fluvial deposits, lacustrine beds and diatomite deposits indicate the presence of standing water. Changes in topography, likely a consequence of the Columbia River Basalt eruptions, would affect the path of local watercourses and may have blocked them completely at times. One hypothesis explaining fast accumulation of lacustrine and fluvial sediments is the formations a temporary lake (or lakes) by drainage blockage. However, fossils are more commonly found in the paleosols of the Cave Basin site, not the fluvial/lacustrine layers (pers. comm., Win McLaughlin), indicating the lake(s) did not fill the entire basin.

SYSTEMATIC PALEONTOLOGY

Class MAMMALIA

Order RODENTIA

Family SCIURIDAE de Waldheim, 1817

Subfamily SCIURINAE de Waldheim, 1817

Tribe PTEROMYINI Brandt, 1855

Genus *BLACKIA* Mein, 1970

Blackia sp.

Figure 4 D-E and Appendix 1

Referred Specimens- Lower first or second molar: UOMNH F-69123. Lower third molar: UOMNH F-69118.

Locality- UO 4343 Cave Basin.

Description- The $M_{1/2}$ is rhomboidal in shape and moderately worn. Despite the wear, fine crenulations can still be observed in the talonid basin. The metaconid is partially broken, but still the tallest cusp. An anterolophid slopes smoothly from the metaconid to a position just anterolingual to the protoconid. There is no terminal anteroconulid, but a slight depression separates the anterolophid and the protoconid. The protoconid is extended lingually slightly, forming a minute metalophid that does not connect to the metaconid. The ectolophid is level with no mesoconid present, connecting midway up both the protoconid and hypoconid. The hypoconid is posterolingually expanded and its posterior edge is curved lingually. The posterolophid connects low on the hypoconid, but rises gently to join the remnants of the entoconid. The posterolingual margin of the tooth is the most worn. While the rise of the entoconid is evident, its true height and morphology, as well of that of the mesostylid, cannot be determined at this stage of wear. The posterlophid dips slightly anterior to the entoconid before rising steeply to connect with the metaconid.

The M_3 is sub-triangular and unworn. The metaconid is the tallest cusp, joined by the anterolophid midway up its height. The anterolophid forms a thin, level ridge. At the lingual edge of the protocone, an extremely thin lophulid connects the anterolophid and protoconid. Buccal to this lophulid, the anterolophid rapidly loses height before smoothly joining the anterobuccal corner of the protocone. A small basin is formed between the anterolophid, lophulid, and anterior face of the protoconid. The protoconid itself is elongated buccally. A low, thin, and incomplete metalophid extends from its lingual side, forming the posterior margin of the trigonid basin. A wide, but moderately tall ectolophid with no mesoconid is set in from the buccal margin of the tooth. It connects to both the protoconid and hypoconid two-thirds of the way up both the cusps. The hypoconid is the widest cusp on the tooth, taking up the buccal half of the posterior portion of the tooth. A slight dip separates the hypoconid from the posterolophid. After this the posterolophid rises and expands to form a significant entoconid of the same height as the protoconid and hypoconid. The posterolingual margin of the tooth bulges outward, with the entoconid forming a slight corner. Notches on either side of the mesostylid separate it from the entoconid and metaconid. A short marginal lophulid anterior to the mesostylid rises to connect low on the metaconid.

Differential Diagnosis and Discussion- The wrinkled enamel in the talonid basins of these teeth indicate affinities with the Pteromyini. Their small size and crenulate (not lophulate) texture (see fig. 2) separate it from *Miopetaurista* (Mein, 1970). These teeth have no mesoconid, ruling out inclusion within *Petauristodon* (Essenger, 1979). These teeth are similar to *Sciurion* in size and crenulation of the talonid basin but lack the mesoconid characteristic of the genus (Skwara, 1979). In addition, *Sciurion* possesses an anteroconid separated from the protoconid by a thin, ravine-like, undeveloped trigonid basin. The Cave Basin M_3 has a well-developed anterolophid, but it has no terminal conulid. The anterolophid is connected to the protoconid by a thin saddle of enamel forming the marginal edge of a trigonid basin significantly larger than that of *Sciurion*. The anterolophid of the $M_{1/2}$ is more closely appressed to the protoconid, but still shows no sign of a terminal conulid.

These teeth match descriptions of *Blackia* (Mein, 1970). *Blackia* lacks a mesoconid and anteroconid according to the generic description ("Les molaires inférieures… dépourvues de mésoconide et d'antéroconide," Mein, 1970, pg. 44) yet *B. miocaenica* has an anterolophid and an anterobuccal re-entrant ("Les molaires inférieures ont un cingulum antéro-externe et un antérosinuside," Mein, 1970, pg. 45). The anterolophid is seen in images of *Blackia* in the defining manuscript, however the degree to which the lophid is developed is variable.

Despite recent opinions that North American *Blackia* material is actually *Sciurion* (Goodwin, 2008), there are key differences between the two genera. *Blackia* has no mesoconid, but does have an anterobuccal re-entrant without an anteroconid on the anterolophid. *Sciurion* has a mesoconid and a low anteroconid on the anterolophid, but no expansion between the protoconid and anterolophid forming an anterobuccal re-entrant. The Cave Basin teeth display a character combination consistent with *Blackia*. While *Blackia* has been described in North American faunas, no species-level identifications have been made. Currently, specific distinctions in European faunas are based on size, not morphology (de Bruijn, 1997). Until a revision of *Blackia* considering all material has been completed, these teeth can only be identified to the generic level.

Genus *PETAURISTODON* Essenger, 1979

Petauristodon sp.

Figure 4 A-C and Appendix 1

Previous Names- *Sciuropterus* Cuvier, 1825.

Referred Specimens- Lower third molar: UOMNH F-69027, F-69109. Upper first or second molars: UOMNH F-64923.

Locality- UO 4343 Cave Basin.

Description- F-69027, an upper first or second molar, is robust with tall, thin crenulations on the buccal portion of the talonid basin. The tip of the metaconid is broken, but the cusp is easily the tallest on the tooth. The buccal edge of the metaconid is elongated and slopes into the anterolophid. Anterolingual to the protoconid, the anterolophid widens to form an anteroconid that is connected to the protoconid by a small lophulid. The anterolophid resumes traveling buccally after the anteroconid, losing height quickly before joining low on the anterobuccal face of the protoconid. The anterolophid is situated close to the protoconid at the buccal edge of the tooth, preventing the formation of an anterobuccal re-entrant. The protoconid has a large, buccally expanded footprint but the tip of the cusp is situated well in from the buccal margin of the tooth. A low, short, and incomplete metalophid is incorporated into the crenulations on the basin of the tooth. A low U-shaped ectolophid connects the protoconid and hypoconid. The mesoconid extends buccally to just short of the tooth's buccal margin. The hypoconid is posterolingually extended. The posterolophid travels anterolingually from its smooth junction with the hypoconid. A small notch forms the posterior edge of the entoconid, while its anterior edge is marked by a sharp drop to the level of the talonid basin. A prominent mesostylid is somewhat anteriorly extended, but separated from the metaconid by a small notch.

F-69109 is slightly smaller and has less prominent crenulations in the talonid basin than F-69027. While the anterolophid rises to form a conulid, it is unconnected to the protoconid and still does not form an anterobuccal re-entrant. The metalophid is more robust, but still incomplete. The ectolophid is more V-shaped than U-shaped and the mesoconid extends fully to the buccal margin of the tooth. The hypoconid is proportionally more posterolingually elongated than F-69027, but the morphology of the posterolophid and entoconid are the same.

F-64923 has relatively smooth enamel compared to the lower third molars. The protocone is positioned near the anterior edge of the lingual margin of the tooth. The anteroloph exits low on the anterior face of the protocone, traveling anteriorly before turning sharply buccally. The anteroloph rises in height and swells, forming an elongated anteroconid. While part of the anteroconid is broken, it is separated from the paracone. The paracone has a triangular footprint and is lingually extended. The protoloph constricts on each side of the protoconule. The mesostyle is large and connected to the paracone on the posterior side of the paracone. The mesostyle is separated from the metacone. The metaloph is constricted at its junction with the metaloph. The metaloph constricts again both before and after the metaconule. Both the metaloph and protoloph travel anterolingually across the tooth. Between the metaconule and protoconule are two transverse valleys that define the edges of the small accessory loph. The posteroloph is low and the posterior valley shallow. In line with the protocone, the posteroloph makes a sharp right turn anteriorly and greatly widens to form a hypocone.

Differential Diagnosis and Discussion- The two lower third molars are referred to *Petauristodon* based on the crenulated basins, buccally elongated mesoconids, and lack of anterobuccal re-entrants. Despite these genus-level similarities, these teeth have significant differences. F-69027 is slightly larger and more robust than F-69109, has a larger entoconid and mesoconid, and has a small lophule connecting the anterolophid to the protoconid. F-69109 has a more delicate, V-shaped ectolophid and a larger hypoconid. While this could conceivably be due to interspecific variation, it could also be intra-specific variation.

While the presence of an accessory loph between the protoloph and metaloph is generally considered characteristic of the upper dentition of *Petauristodon* (Essenger, 1979), it is also present in some species of *Miopetaurista* (Mein, 1970 and de Bruijn, 1980). However, it can be a useful diagnostic character when seen in conjunction with other characters. *Petauristodon* has more prominent conules on the $M^{1/2}$ than *Miopetaurista* and appears to lack the lophules that can diverge from the protoloph and especially the metaloph in *Miopetaurista* (see Mein (1970) figures 15, 16, and 17 (*M. lappi*), 22 (*M. guillardi*), 29 and 30 (*M. crusafonti*) and 35, 40, and 41 (*M. thaleri*); see also Casanovas-Vilar (2015) figure 1b (*M. crusafonti*)). The Cave Basin tooth has both a protoconule and a metaconule and a poorly developed lophule between the metaloph and protoloph, but no lophules extending off the protoloph or metaloph.

This specimen is too large to be a member of *Petauristodon minimus* (Anteroposterior: 0.95-0.96 mm. Transverse: 1.14-1.16 mm. (Lindsay, 1972)). Conversely, *Petauristodon pattersoni* is too large (Anteroposterior: 3.39 mm. Transverse: 2.78 mm. (Pratt and Morgan, 1989). *Petauristodon jamesi* appears to have more lophulate enamel and *Petauristodon mathewsi* has more defined crenulations than the Cave Basin *Petauristodon* (James, 1963 and Lindsay, 1972). *Petauristodon uphami* has no known lower molars, but the upper molars have a beaded texture not seen on the Cave Basin *Petauristodon* (James, 1963). While the Cave Basin material appears different from other described species of *Petauristodon,* distinctions cannot be made at this point given the limited amount of material present.

Genus *MIOPETAURISTA* Kretzoi, 1962

cf. Miopetaurista

Figure 4 F-I and Appendix 1

Previous Names- *Cryptopterus* Mein, 1970.

Referred Specimens- Upper fourth premolar: UOMNH F-69068. Upper first or second molar: UOMNH F-69117. Upper third molars: UOMNH F-69119, F-69120.

Localities- UO 4343 Cave Basin, UO 4343 Cave Basin, UO 4343 Cave Basin.

Description- The P_4 is triangular with lophulate enamel. The anteroloph does not join the protocone, leaving the anterior valley open on the lingual side. The anteroloph rises quickly to form a tricuspid anterocone. Notches in the enamel separate the three conules of the anterocone. The anteroloph does not continue after the anterocone and the anterior valley is open buccally. The paracone is lingually shifted, leaving behind a prominent shelf-like buccal cingulum. The paracone has a triangular footprint when viewed from the occlusal surface and is arrowhead-shaped when viewed from the buccal edge of the tooth. The protoloph runs straight across the tooth joining the protocone without constriction. There is no protoconule, but at the very buccal end of the protoloph, a multi-branched lophule runs posterolingually towards the protocone. The mesostyle is large and situated on the buccal margin of the tooth. It is triangular, pointing towards the interior of the tooth, and constricts slightly before forming a short lophule. The posterobuccal edge of the tooth is broken. The metaloph runs posterobuccally shortly before splitting into a large metaconule and a posteriorly curving metalophule. The metalophule surrounds the posterior half of the metacone and rejoins the metaloph with a small secondary metaconule. A low posteroloph curves around the metalophule-metaloph complex before smoothly gaining in height to join the protocone. Despite the limitation of the protocone to the anterior portion of the lingual margin of the tooth, the hypocone is barely developed and only created by a small transverse swell in the posteroloph.

The $M^{1/2}$ is highly worn with little original enamel remaining. What does remain depicts a quadrate tooth with lophulate rugosity in the anterior valley and the valley formed by the protoloph and metaloph. One lophule appears to join the buccal end of the protoloph and extend lingually. Irregular wear of blocky lophules complicates the description of the teeth. Worn lophule near the buccal margin of the tooth may depict a lingually elongated mesostylid that constricts before widening to form another worn lophule indicating a second metaconule. There is a deep ravine between the first, most lingual and largest metaconule and the posterolophid. No protoconule or its remains are visible, but a lophule ran anteriorly out of the protoloph, shown by the worn remains of the enamel.

The M^3s are both missing their posterior lobe. The protocone is large and occupies the entire lingual border of the tooth. The anteroloph smoothly slopes down form the top of the protocone and curving gently around the anterior face of the tooth. A small notch is present before it joins the large, somewhat triangular paracone. A small lophule exits the posterolingual face of the paracone, running posteriorly. However, it does not seem to be a mesostyle or connect to a mesostyle. The protoloph slopes gently as it travels lingually, appearing beaded when unworn and more lophulate when worn. A small protoconule is present. On F-69120, a lophule extends anterobuccally from the protoconule. On F-69119, a lophule exits the protocone and runs anteriorly before sharply curving buccally around the protoconule. The metalophule exits the protocone close to the protoloph and quickly constricts. A large metaconule is present and connects to the posterolingual margin of the tooth via an irregularly shaped lophule. The metaloph does not continue buccally. Instead, on F-69120 (which is slightly less broken than F-69119), the basin is filled with many irregularly pattered lophules.

Differential Diagnosis and Discussion- These teeth represent the largest sciurid found at Cave Basin. The P^4 and $M^{1/2}$ lack the hypocone, accessory lophules, and distinct protoconule characteristic of *Petauristodon* (although the metaconule is well-developed). The presence of other non-*Petauristodon*-like lophules is typical of *Miopetaurista*. The M^3 has lophules extending posteriorly from the metaconule, a character of *Miopetaurista* that separates it from *Petauristodon*.

Identified specimens of *Miopetaurista* in North America are extremely rare. Prior to this, only two instances have been found, both from the Pliocene of Florida. These Floridian specimens represent the only North American *Miopetaurista* species, *M. webbi*. Originally identified as *Petauria* (Robertson, 1976), the specimens were recently reassigned to *Miopetaurista* (Webb, 2008).

The abrupt reappearance of *Miopetaurista* in the Pliocene of Florida should be surprising- if these squirrels are in fact related to the European genus. Large geographic and temporal gaps separate this genus from its European and Asian affiliates. It is unlikely that taphonomy strongly influenced the lack of *Miopetaurista* seen in the North American fossil record of forested regions. Modern taphonomic studies indicate that bone fragments can persist on forest floors and that shade and humidity may actually slow and reduce fragmentation by weathering processes (Kerbis Peterhans, 1993 and Tappen, 1994). While forest environment fossils are proportionally underrepresented in the fossil record, environmental conditions are unlikely to be destroying the teeth before they can be preserved. The dearth of *Miopetaurista* could reflect their actual abundance in forest communities. *Cf. Miopetaurista* accounts for 2% of the squirrel teeth recovered from Cave Basin. In general, the Pteromyini are rare in the fossil record compared to other Sciurid taxa. *Miopetaurista* may be sparsely distributed across the landscape. Alternatively, *Miopetaurista* fossils may have been misidentified, as was the case with a large P^4 originally published as *Sciuropterus* and catalogued as *Protospermophilus malheurensis* (UOMNH F24390, UO 2495 Red Basin) (Shotwell, 1969). The presence of *cf. Miopetaurista* in the Cave Basin fauna indicates careful and thorough sediment screening will collect rare taxa if they are present at a site.

American *Miopetaurista* still represent a biogeographical conundrum. It is easier to accept a mid-Miocene occurrence of *Miopetaurista* than a Pliocene occurrence. However, the presence of North American *Miopetaurista*, in spite of the differences in their ages, allows us to geographically link the Floridian and Eurasian occurrences. The transcontinental migration of North American flying squirrels has been and still continues to be of interest to biogeographers. While eastward migration is the prevailing hypothesis, modern molecular phylogenies support the evolution of extant flying squirrels from New World tree squirrels (Sciurini), indicating a westward migration (Steppan, 2004). However, other molecular and morphological phylogenies still report eastward migrations (Lu, 2013 and Oshida, 2000). Regardless of the directionality of the migration, the genetic relationships of modern New and Old World flying squirrels suggest Pteromyini were able to cross the Bering Strait land bridge. The older age of European *Miopetaurista* and very young age of the Floridian *Miopetaurista* support an eastward migration out of Europe.

The eastward migration hypothesis allows us to predict that we would find *Miopetaurista* fossils in Asia and North America during the Miocene (and perhaps Pliocene) as the squirrels emigrated. In line with this prediction, occurrences of the genus are reported from east Ukraine, south-eastern Russia, eastern Kazakhstan, south-central, north-eastern and the central coast of China, (Agadjanian, 2010 (abstract), Li, 1983, Shevyreva, 2003, and Qui, 2002 and 2003). Occurrences of fossil Sciuridae in north-eastern Russia, Alaska, the Yukon Territory and British Columbia (Canada) are sparse and limited to the Pleistocene and Holocene (Paleobiology Database, accessed on 24 June 2013, search terms: Sciuridae, Pteromyinae, *Miopetaurista*). Further occurrences of *cf. Miopetaurista* are limited to the Cave Basin material and possibly the Red Basin material; however, the material from these North American sites are still only tentatively referred to the genus. While the presence of *cf. Miopetaurista* in the Miocene of Oregon is biogeographically logical, it is the first material of Miocene age to be published as *cf. Miopetaurista* and represents a continental range extension of 10 MA. More identification and discussion of large, North American flying squirrels must occur before definitive statements can be made about their relationship with European flying squirrels.

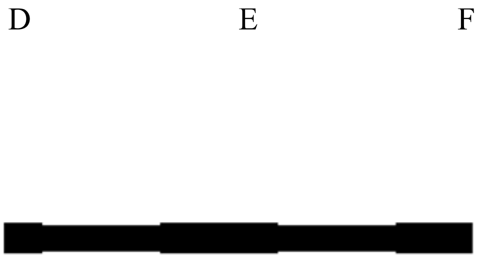

Figure 4. The Pteromyini of Cave Basin

Petauristodon: A. UOMNH F-69027. B. UOMNH F-69109. C. UOMNH F-64923. *Blackia*: D. UOMNH F-69118. E. UOMNH F-69123. *cf. Miopetaurista* : F. UOMNH 69068. G. UOMNH 69117. H. UOMNH 69119. I. UOMNH 69120.

Tribe MARMOTINI (Pocock, 1923)

Genus *MIOSPERMOPHILUS* Black, 1963

Miospermophilus paulinaensis

Figure 5 and Appendix 1

Holotype- Lower first or second molar: UOMNH F-64919.

Paratypes- Lower fourth premolar: UOMNH F-64914. Lower third molar: UOMNH F-64960. Upper fourth premolar: UOMNH F-69124. Upper first or second molar: UOMNH F-64901. Upper third molar: UOMNH F-69083.

Referred Specimens- Lower fourth premolars: UOMNH F-64909, F-64937, F-69103. Lower first or second molars: UOMNH F-64908, F-64911, F-64936, F-64950, F-64954, F-64958, F-69081, F-69115. Lower third molars: UOMNH F-64955, F-64961, F-69127. Upper fourth premolars: UOMNH F-64913, F-64943, F-64959. Upper first or second molars: UOMNH F-64903, F-64906, F-64907, F-64929, F-64945, F-64948, F-64952, F-69075, F-69094, F-69095. Upper third molars: UOMNH F-64924, F-69104, F-69108.

Localities- UO 4343 Cave Basin, UO 4343 Cave Basin.

Diagnosis- Very quadrate upper molars; protocone not extended across lingual margin of tooth; antero- and postero- lophs distinct from protocone on lingual margin; metaloph moderately constricted lingual to metaconule; posterointernal corner of M_3 expanded and has a strong notch between the protoconid and anteroloph; entoconid region rounded; entoconid prominent; anterolophid anteriorly expanded sometimes forming anteroconulid; trigonid basin more distinct than *M. wyomingensis*.

Etymology- Named for Paulina, Oregon, the closest town to the Cave Basin localities.

Description- P_4 is sub-quadrate. The metaconid is the tallest cusp and closely appressed to the protoconid. A small notch separates the two cusps. In one specimen, a minute anteroconid is present, but most specimens have no anteroconid. A low ectolophid bridges the short distance between the protoconid and the buccally shifted hypoconid. The posterolophid tends to extend slightly further posteriorly past the hypoconid before smoothly circling to join the base of the metaconid. The enamel is raised slightly on the posterolingual corner, indicating an entoconid.

The $M_{1/2}$ has relatively high cusps and lophs. The metaconid is the tallest cusp. An anterolophid slopes steeply down from the metaconid, often being subdivided into two cuspulids and ending anterior to the protoconid. A metalophid may extend off the protoconid and join the metaconid. This feature is variable and may be a difference between the M_1 and M_2, although it is impossible to say without an associated dentition. The ectolophid is low and set back from the margin of the tooth. A mesoconid is present and may extend labially. The hypoconid is round and the posterolophid exits midway up its posterolingual face. The posterolophid curves around the posterolingual margin without a sharp corner. The entoconid is peg-like and shifted anteriorly (in comparison to other sciurids). A notch divides the entoconid from the mesostylid, which then rises immediately and steeply to the metacone.

The M_3 is sub-quadrate in shape and low-lophed, although the cusps themselves can be quite tall. The metaconid is the tallest cusp, steeply but smoothly dropping to form an anterolophid ending just anterior to the protoconid. In some specimens, a small notch separates the anterolophid and protoconid. In others, the anterolophid joins the protoconid. A small metalophid slopes off the protoconid towards the midpoint of the anterolophid, forming a small pit between the lophids and the protoconid. A small mesoconid is present on the low ectolophid. The hypoconid is elongated and bean-shaped. The posterolophid exits the hypoconid at the maximum height of the cusp and briefly travels lingually before making a sweeping curve towards the metaconid. A minute hypoconulid appears present on some specimens, but appears to have been lost with wear on others. It is closely appressed to the broad, low entoconid. A small notch separates the entoconid from the mesostylid. The enamel gains height quickly after the mesostylid to form the metaconid. None of the posterolingual features break the smooth curve of the posterolingual margin.

The P^4 is sub-triangular, yet molariform. The anteroloph is low, lining the edge of a small round ledge of variable depth. The anteroloph connects low on both the paracone and the anterior face of the tooth. The protoloph connects smoothly to the protocone. The metaloph is generally constricted where it joins the protocone forming one edge of the metaconule. No mesostyle is present. The posteroloph exits low on the lingual face of the metacone and curves around the metaconule before joining the protocone.

The $M^{1/2}$ is quadrate. The protocone is elongated but does form the whole lingual margin of the tooth. The anteroloph exits midway up the anterior margin of the protocone, briefly traveling anteriorly before turning sharply and running buccally. The anteroloph then turns lingually before ending. It does not join the paracone. The protoloph connects smoothly to both the protocone and paracone. No protoconule is present. A small mesostyle is present and may be shifted slightly buccally in some of the molars. The metaloph is somewhat constricted at the protocone and the metaconule is rarely further developed. The posteroloph exits low on the posterobuccal face of the metacone, running directly buccally until just posterior to the protocone. At this point it sharply turns anteriorly and joins midway up the protocone. In many of the teeth, the posteroloph descends before rising to join the protocone, denoting a small hypocone.

The M^3 is triangular. The protocone forms the majority of the lingual margin of the tooth. The anteroloph joins the anterocone on the anterior face of the tooth and gently gains in height until it joins the anterior face of the paracone. The protoloph exits the lingual face of the protocone and dips before rising to join the paracone. No metacone or metaloph is present. The posteroloph exits low on the parastyle, traveling posteriorly before circling back around to smoothly join the protocone. An extremely low mesostyle is present at the posterior base of the paracone.

Differential Diagnosis and Discussion- These teeth belong to the smallest member of Marmotini at Cave Basin. Members of the Pteromyini can be ruled out by the absence of rugose enamel. These teeth are larger and more complex than the *Tamias* found at Cave Basin. Specimens assigned to *Miospermophilus paulinaensis* have some general characteristics of *Miospermophilus*, like rhomboidal proportions in the lower teeth and ectolophids that are well-set in from the buccal margin (Black, 1963). Compared to other genera, the entoconids are small and not expanded across the posterolophid (another characteristic of *Miospermophilus*).

Miospermophilus paulinaensis displays features of both *M. wyomingensis* and *M. bryanti*, complicating its initial identification. *M. paulinaensis* differs from *M. wyomingensis* in the smaller metaconules and less constricted metaconules, the presence of an entoconid in a rounded (not angular) posterolophid, and the increased development of the anterolophid. *M. paulinaensis* differs from *M. bryanti* in the quadrate shape of the upper molars, the decreased size of the protocone, and the presence of an anterolophid, and the notch between the protoconid and metaconid on P_4. *M. paulinaensis* differs from *M. lavertyi* in the presence of a metaconule and slight constriction of the metaloph before it reaches the protocone, the consistently larger and more anteriorly placed anterolophids, and the more marginal placement of the ectolophid (Dalquest, 1996). Given the lack of morphologically consistent *Miospermophilus* species, I propose *M. paulinaensis* as a new small species in the Marmotini.

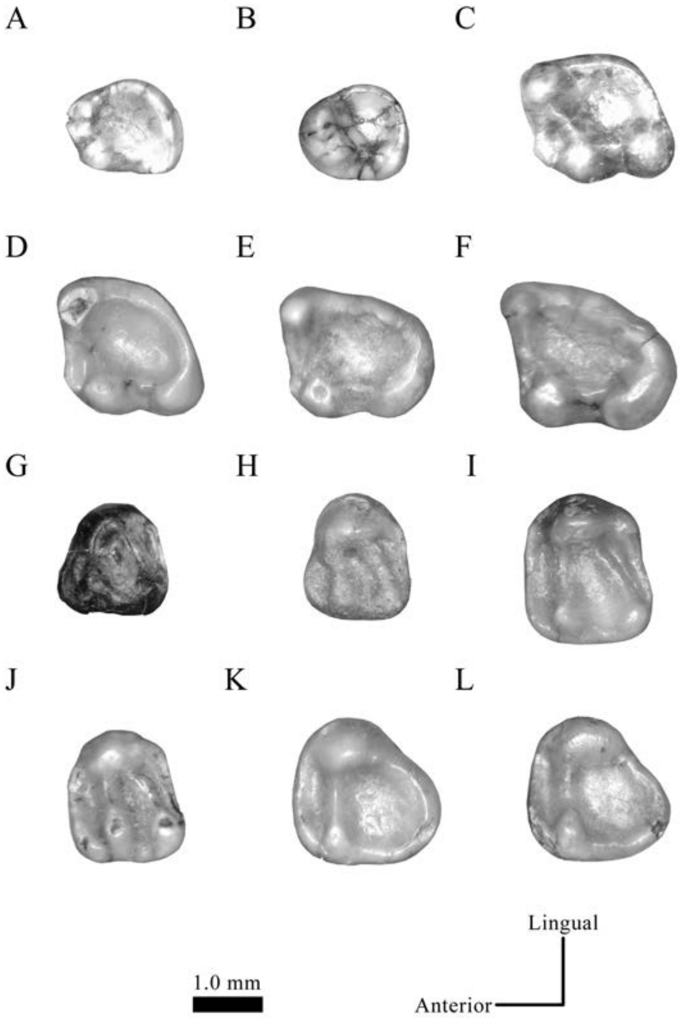

Figure 5. *Miospermophilus paulinaensis* from Cave Basin

A. UOMNH F-64909. B. UOMNH F-64914. C. UOMNH F-64919. D. UOMNH F-69081. E. UOMNH F-69127. F. UOMNH F-64960. G. UOMNH F-64959. H. UOMNH F-69124. I. UOMNH F-64907. J. UOMNH F-64901. K. UOMNH F-69083. L. UOMNH F-69104.

Genus *PROTOSPERMOPHILUS* Downs, 1956

Revised diagnosis- As described by Black (1963), except state of protoconule is not diagnostic of genus; protoconule may be absent or subordinated in protoloph or fully present as in P. oregonensis; hypocone may be present in some species.

Protospermophilus oregonensis

Figure 6 and Appendix 1

Arctomyoides oregonensis Downs, 1956: pp. 179-181, plate 14 figure 1.

Referred Specimens- Lower fourth premolars: UOMNH F-64965, F-64966, F-64971, F-64975, F-64977, F-64990, F-64998, F-69053, F-69059, F-69064, F-69079, F-69085, F-69138, F-69145, F-69177, F-69194. Lower first molars: UOMNH F-64978, F-64983, F-64991, F-64994, F-69022, F-69023, F-69030, F-69035, F-69061, F-69067, F-69157, F-69168, F-69182, F-69184. Lower second molars: UOMNH F-64980, F-69040, F-69050, F-69056, F-69142, F-69143, F-69151, F-69152, F-69164, F-69170, F-69196, F-69200. Lower third molars: UOMNH F-64970, F-64988, F-64989, F-64997, F-69049, F-69057, F-69062, F-69116, F-69153, F-69172, F-69173, F-69181, F-69187, F-69207, F-69208. Upper fourth premolars: UOMNH F-64973, F94981, F-64986, F-64987, F-69017, F-69031, F-69043, F-69052, F-69060, F-69140, F-69147, F-69186, F-69197. Upper first or second molars: UOMNH F-64967, F-64969, F-64972, F-64976, F-69024, F-69025, F-69026, F-69029, F-69033, F-69036, F-69041, F-69047, F-69051, F-69058, F-69066, F-69139, F-69146, F-69148, F-69149, F-69154, F-69156, F-69158, F-69161, F-69176, F-69178, F-69183, F-69185, F-69188, F-69189, F-69192, F-69193, F-69195, F-69198, F-69204, F-69205, F-69206. Upper third molars: UOMNH F-69019, F-69021, F-69028, F-69046, F-69054, F-69141, F-69160, F-69163.

Localities- UO 4343 Cave Basin CAVE BASIN, UO 4343 Cave Basin, UO 4343 Cave Basin.

Description- The P_4 is sub-quadrate and molariform. The metaconid is taller than the protoconid and a low, saddled metalophid connects the two cusps. An anteroconid is situated anterior to the metalophid. The anteroconid is variable, but appears on most of the P_4 specimens. It is absent in other teeth or attached to the protoconid as an anterolophid. The mesostylid is small, but separate from both the metaconid and entoconid. The entoconid is well developed, separated from a strong posterolophid by a notch. The posterolophid slopes to join the hypoconid. A small hypoconulid may be present in some specimens, but many of the posterolophids are worn and do not show this cusp. The posterobuccal margin of the tooth is expanded buccally and the hypoconid is large but low. The mesostylid sits on a well-developed V-shaped ectolophid connecting smoothly to the protoconid and hypoconid. A large ectostylid is present in a minority of specimens.

The M_1 and M_2 are rhomboidal. The posterior margin of the tooth is heavy, ending labially with a hypoconulid separated from the hypoconid by a small notch. The posterolophid is capped lingually with a large entoconid. The entoconid and mesostylid are separated almost to the floor of the talonid basin. The mesostylid may be more closely appressed to the metaconid or separated from it by a small notch. The mesoconid is set in from the labial margin of the tooth in a V-shaped ectolophid that connects low on the side of both the protoconid and hypoconid. A minute ectostylid may be present at the base of the hypoconid, labial to the connection of the ectolophid.

The M_1 and M_2 differ in metalophid and anterolophid/anterocone morphology. The M_1 has a more peg-like anterocone that is separate from the metaconid. The metalophid is low but complete, separating the talonid basin from a trigonid basin. In contrast, the anterolophid of M_2 is elongated and connects low on the metaconid. The metalophid extends as if to connect to the metaconid, but ultimately is incomplete at the base of the metaconid. The M_2 is also larger than the M_1.

The M_3 is triangular. The posterobuccal margin of the tooth is dominated by the elongated hypocone. An enlarged posterolophid dominates the posterolingual margin of the tooth. A small hypoconulid may be present. If it is, it is posterior to a shallow vertical groove. An elongated entoconid is anterior to the groove and separated from a low mesostylid by a small notch. The mesostylid is separated from the metaconid by a small notch. A smoothly sloping anterolophid connects to the metaconid, forming the anterior margin of the tooth. This anterolophid is variably developed labially. In unworn specimens, it appears moderately to strongly separate from the protoconid, but appears to connect directly to the protoconid in worn specimens. The protoconid slopes gently to the floor of the tooth, but does not form a connected metalophid. The trigonid basin is an open valley situated between the anterolophid and the protoconid. The mesoconid is set in from the labial margin of the tooth in a V-shaped ectolophid that connects low on the side of both the protoconid and hypoconid. A minute ectostylid may be present at the base of the hypoconid, labial to the connection of the ectolophid.

The P^4 is robust and sub-quadrate. The protocone is expanded across the lingual margin of the tooth, but its highest point is situated anteriorly within the cusp. The anteroloph is low, but rises into a bulging anterocone. The paracone is roughly the same height as the protoconid and metaconid. The protoloph trends anterobuccally and may connect smoothly to both the protocone and paracone or may barely constrict before it joins the protocone. There is no protoconule present. The metaloph also trends anterobuccally but is heavily constricted at its juncture with both the metacone and the protocone. The metaconule is large and can be seen even in heavily worn teeth. A small mesostyle is situated in line between the paracone and metacone. Though frequently worn, it is visible even in teeth with late stage wear. The posteroloph is thick, beginning low on the metacone before rising slightly as it curves around the metaconule and joins the posterior edge of the protocone.

The $M^{1/2}$ is a robust and quadrate tooth. Compared to other *Protospermophilus* species, the protocone is reduced and only fills the middle portion of the labial margin. The posterolingual and anterolingual face of the protocone is marked by one to three vertical indents in the enamel. The anteroloph exits low on the posteroloph, traveling slightly anteriorly before turning sharply buccally. The anterolophid gains height, forming an anterocone before dropping steeply. If the anteroloph curves posteriorly towards the paracone, it either does not join the paracone or joins very low on the buccal edge of the cusp. While the paracone is unremarkable, the protoloph is highly variable. The protoloph typically slopes smoothly out of the paracone, running straight across the tooth with little protoconule development or constriction at the protocone. Although less common, the protoloph may join the paracone midway up the lingual face of the cusp and travel posterolingually before jogging anterolingually. The protoloph may constrict several times, displaying a large protoconule and several incorporated accessory conules. In this condition, the protoloph is generally constricted where it meets the protocone. While these seem like very different conditions, intermediate conditions are common, as the characters exist on a gradient between the described extreme conditions. A mesostylid is situated between or occasionally buccal to the paracone and metacone. It is often anteroposteriorly expanded and sometimes is conjoined with the paracone. The metacone and metaloph are more predictable. The metaloph joins the metacone near its peak and travels slightly posterolingually. It constricts and then widens, forming an anterolingually trending elongated metaconule. The metaconule is partly constricted or fully incomplete where it joins the protocone. The posterolophid exits low on the posterolingual face of the metacone, traveling lingually until just buccally of the protocone. Here, it turns sharply anteriorly and swells, forming a hypocone. The hypocone may be smoothly appressed to the protocone or a notch may separate the two cusps. Generally, larger protoconules are seen in conjunction with more separate distinct hypocones. However, this is not the rule and the features are independently variable.

The M^3 is robust. The protocone is typical of *Protospermophilus* and occupies the lingual margin of the tooth. A low anteroloph connects smoothly to the protocone and ends at the labial margin of the tooth. The anterocone is separated from the paracone. The paracone is the same height as protocone and connected to it by a gently sloping protoloph. In unworn or lightly worn specimens, a protoconule is formed by a slight constriction before the protoloph joins the protocone. A small mesostyle is present and separated from the posteroloph by a small notch. However, any wear erases this feature. The posteroloph forms the rounded labial margin of the tooth and smoothly joins the protocone.

Differential Diagnosis and Discussion- The lower teeth have similar proportions to *Protospermophilus oregonensis*. The size of the Cave Basin sample shows that variation in the dimensions of *P. oregonensis* teeth is greater than previously thought and extend past the lower limit of previously reported values. The lower teeth are larger than the teeth of *Protospermophilus angusticeps*, *Protospermophilus quatalensis*, *Protospermophilus kellogii*, and *Protospermophilus vortmani*. Although the lower molars of *Protospermophilus. malheurensis* have not been described, its upper dentition is smaller than *P. angusticeps*. It is probable that the lower dentition of *P. malheurensis* will also be smaller than *P. angusticeps,* indicating the Cave Basin *Protospermophilus* do not belong to *P. malheurensis*.

Morphologically, these teeth strongly resemble *P. oregonensis*. The M_3s have the faint vertical posterolingual groove diagnostic of *P. oregonensis* (Downs, 1956). However, contradicting Black (1963), a mesostylid is nearly always present to some degree on the M_3. These M_3s are slightly smaller than reported dimensions of *P. oregonensis* (Black, 1963). However, minor dwarfism in other taxa has been reported at the nearby Mascall Formation site, Hawk Rim (McLaughlin *et al.*, 2016). The M_1 and M_2 have small hypoconulids, anterolophids and/or anteroconids, and a prominent valley between the anterior margin of the tooth and the metalophid. This combination of characters is diagnostic of *P. oregonensis*.

However, the prominent protoconule on the upper molars does not fit within the genus definition of *Protospermophilus* as given by Black (1963). All other *Protospermophilus* species lack or have an incipient protoconule. Additionally, the protoconule tends to be poorly developed or absent in other North American Sciuridae, except for *Petauristodon.* However, the Cave Basin teeth do not have the accessory lophs or crenulate enamel of *Petauristodon*. In addition, these teeth are larger than the *Petauristodon* specimens found at Cave Basin. Other than the protoconule, these teeth appear to fit the genus-level characters of *Protospermophilus*. Above I amend the diagnostic characters of *Protospermophilus* to include the variation of protoconule states seen in *P. oregonensis* and other species within the genus.

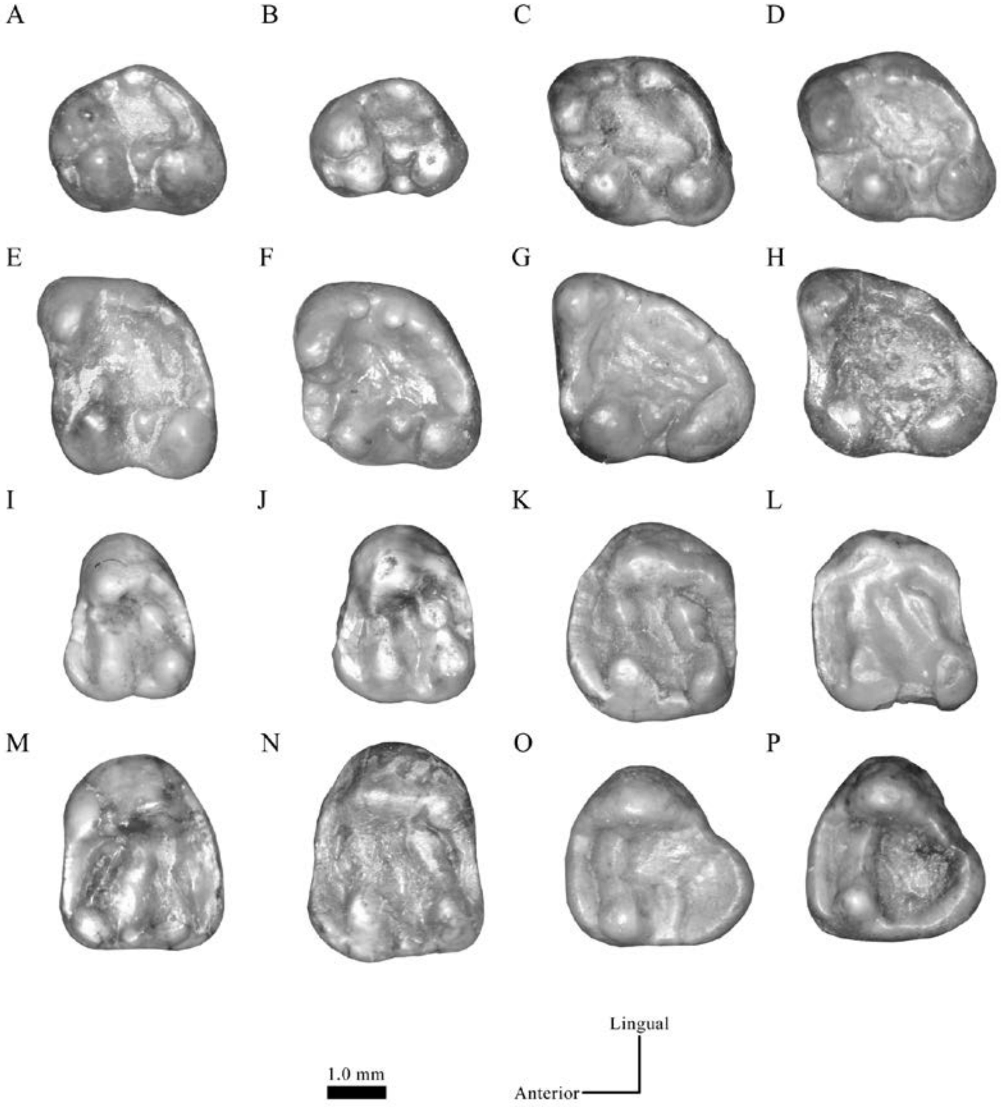

Figure 6. *Protospermophilus oregonensis* from Cave Basin

A. UOMNH F-64975. B. UOMNH F-69053. C. UOMNH F-69182. D. UOMNH F-69157. E. UOMNH F-69142. F. UOMNH F-69153 G. UOMNH F-69170. H. UOMNH F-69116. I. UOMNH F-69017. J. UOMNH F-69060. K. UOMNH F-69033. L. UOMNH F-69183. M. UOMNH F-69149. N. UOMNH F-69047. O. UOMNH F-69021. P. UOMNH F-69019.

Tribe TAMIINI Weber, 1928

Genus *TAMIAS* Illiger, 1811

Tamias sp.

Figure 7 A-G and Appendix 1

Referred Specimens- Lower fourth premolars: UOMNH F-64947, F-69133, F-69135. Lower first or second molars: UOMNH F-64910, F-69126, F-69130. Lower third molar: UOMNH F-69087. Upper first or second molar: UOMNH F-69134.

Localities- UO 4343 Cave Basin, UO 4343 Cave Basin.

Description- The P_4 is very small and bean-shaped. The metaconid is the highest cusp, followed by the protoconid. The metaconid and protoconid are closely appressed, but separated by a small notch. An anteroconid lies anterior to the protoconid. The ectolophid is barely taller than the floor of the talonid basin. The hypoconid is round, but buccally shifted, which expands the posterior area of the talonid basin. The thin, peg-like entoconid does not disturb the smooth half-circle curve of the posterolophid from the hypoconid to the metaconid. A minute mesostylid may be present.

The $M_{1/2}$ is all well worn, obscuring much of the specific morphology. A small anterolophid is present, separated from the protoconid by a deep groove slash. There is no metalophid or trigonid basin present. The ectolophid is level with no trace of a mesoconid. The hypoconid is small and round. The posterolophid is low and simple, but boasts a well-developed entoconid. The anterior edge of the entoconid may be defined by a notch separating it from the mesostylid.

The M_3 is moderately worn and robust in nature. The anterolingual corner of tooth is broken and no part of the metaconid is present. The anterolophid is low and separated from the protoconid by a shallow depression. The protoconid is roughly teardrop shaped, with the point facing the interior of the tooth. However, there is no real metalophid or corresponding trigonid basin. A low ectolophid with no mesoconid connects the protoconid to the low, broad, bean-shaped hypoconid. The posterolophid is low, rising slightly to form a broad entoconid. The condition of the mesostylid cannot be evaluated due to breakage.

The $M^{1/2}$ is slightly worn, low crowned, and sub-quadrate. The protocone is anteroposteriorly expanded, forming the entire labial margin of the tooth. The anteroloph forms a ledge without an anterocone. The paracone and metacone are the same height. The protoloph is smooth, but the metaloph has a small metacone. There is a small mesostyle present. The posteroloph is low, smoothly curving around the metaconule to join the protocone.

Differential Diagnosis and Discussion- These teeth are not consistent with *Miospermophilus paulinaensis* or *Blackia*, the Cave Basin sciurids closest in size. These teeth are referred to the Tamiini based on their small metaconules and angular posterolingual corners of the lower molars, as those are tribe-level characters according to Black (1963). Within Tamiini, there are three recognized genera and many more taxonomic opinions. While taxonomic revisions include all chipmunks in *Tamias,* some cite the presence of unfused lower molar roots as a defining character of the *Tamias*/*Eutamias* clade and fused lower molar roots as a character of *Nototamias* (Goodwin, 2008). Given the unfused state of intact roots, these teeth are placed within *Tamias*. Species-level assignments cannot be made for *Tamias* based on isolated teeth, so I leave the species indeterminate for now.

Genus *NOTOTAMIAS* Pratt and Morgan, 1989

Nototamias sp.

Figure 7 H and Appendix 1

Referred Specimens- Lower first or second molar: UOMNH F-69121.

Locality- UO 4343 Cave Basin.

Description- This tooth is small, somewhat rhomboidal, and well-worn. The talonid basin has smooth enamel. The metaconid is the tallest cusp, followed by the entoconid. The hypoconid and protoconid are equal in height. As the labial margin of the tooth is the most heavily worn, these observations on height may not be consistent with unworn teeth. There is no evidence of an anterolophid, but this may also be due to the advanced state of wear. The labial margin of the tooth is too worn to describe the morphology of the protoconid, ectolophid, and hypoconid as anything more than squirrel-like. The posterolingual corner rises to form an entoconid, while anterior to that the margin bulges lingually suggesting a mesostylid. The two anterior roots are fused almost to the ends of the roots.

Differential Diagnosis and Discussion- This sciurid was the smallest present at Cave Basin (see Appendix 1 for measurements). While its morphology is too worn to be diagnostic, it is placed within the Tamiini on the basis of size. The fused anterior roots on lower teeth are characteristic of *Nototamias*, while the roots of *Tamias* are unfused (Pratt and Morgan, 1989). However, this tooth is significantly smaller than either *N. hulberti* or *N. quadratus* (Pratt and Morgan, 1989 and Korth, 1992).

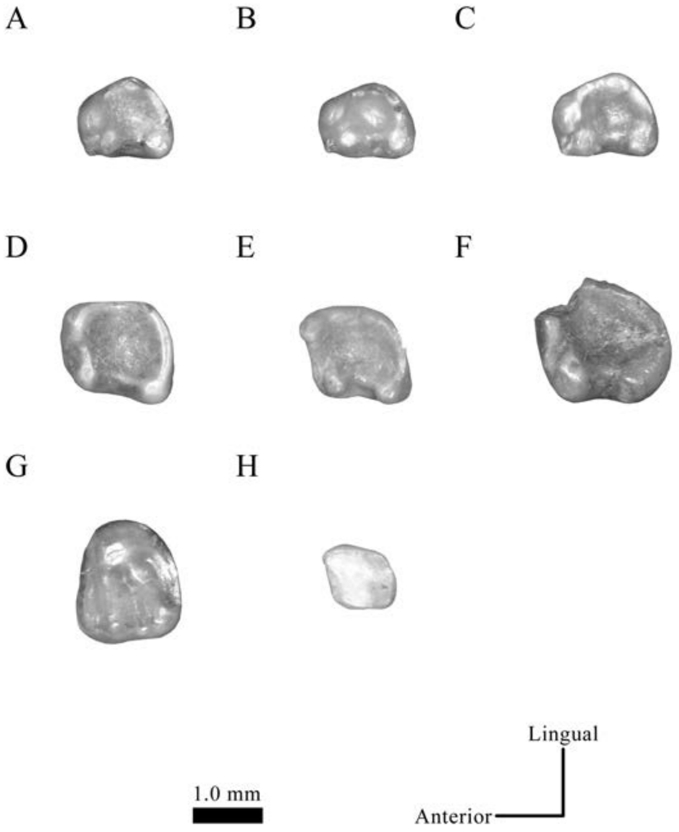

Figure 7. The Tamiini of Cave Basin

Tamias: A. UOMNH F-64930. B. UOMNH F-64910. C. UOMNH F 69087. D. UOMNH F-64947. E. UOMNH F-69133. F. UOMNH F-69135. G. UOMNH F-64134. *Nototamias*: H. UOMNH F-69121.

PALEOECOLOGY

Sciurids are common components of Mid-Miocene microfaunal assemblages and have a robust publication record (Downing, 1992, Downs, 1956, Gazin, 1932, Shotwell, 1968, and Wallace, 1946, among others). The Cave Basin field site has produced sciurid fossils belonging to seven identifiable genera (Table 2). Only the Devils Gate site from the Sucker Creek fauna has produced similar levels of diversity (Downing, 1992). However, Cave Basin displays higher intratribal diversity in the Pteromyini and Tamiini and lower intratribal diversity in the Marmotini. This suggests possible differences in paleoenvironments between the two sites.

Protospermophilus is a common member of mid-Miocene Oregon faunal assemblages. Similarly, *Spermophilus tephrus* is common in mid-Miocene sciurid-containing assemblages. Patterns of co-occurrence of small and large sciurids have long been observed in modern communities. These ecological cohabitation patterns may be preserved within the fossil record as well. Further paleoecological studies of North American Sciurids could test the co-occurrence of *Protospermophilus* species and *Spermophilus tephrus* and the presence of *Miospermophilus* and other large ground squirrels. Regardless, the presence and abundance of the two Marmotini (*Protospermophilus* and *Miospermophilus*) found at Cave Basin indicate the presence of some open habitats.

Contrasting this assessment, the presence of three genera of Pteromyini at Cave Basin indicates a forested environment. Compared to the other faunas discussed, Cave Basin is unique in the diversity of Pteromyini present. Although it has not produced *cf. Miopetaurista* material, both *Blackia* and *Petauristodon* have been reported from Devils

Gate. Red Basin has produced *Petauristodon* and possible *cf. Miopetaurista* remains. Cave Basin’s diversity of Pteromyini indicates there were multiple arboreal niches available to squirrels. Similarly, the presence of two different genera of Tamiini of different size indicates the presence of multiple terrestrial niches.

	Cave Basin	Red Basin	Quartz Basin	Beatys Butte	Sucker Creek-Devils Gate	Mascall Fauna	Skull Spring
Tamias sp.	X				X		
Nototamias sp.	X						
Eutamias sp.		X					
Protospermophilus				X**			
P. oregonensis	X					X	
P. malheurensis		X			X		X
P. quatalensis					X		
Miospermophilus							
M. paulinaensis	X						
Spermophilus							
S. tephrus		X	X		X		X
Citellus							
C. ridgwayi							X
Sciurus sp.				X			
Blackia sp.	X				X		
Petauristodon sp.	X	X			X		
cf. Miopetaurista	X	X*					

* indicates non-published determination from the UOMNCH collections records.
** indicates non-published determination from the UCMP collections records.

Table 3. Faunal comparison of Middle Miocene sciurid assemblages of Oregon

An X indicates presence of that taxon at that site. Red Basin and Quartz Basin data from Shotwell (1968). Beatys Butte data from Wallace (1946). Sucker Creek- Devils Gate data from Downing (1992). Mascall Fauna data from Downs (1956). Skull Spring data from Gazin (1932).

These sciurid taxa indicate an environment with a horizontal environmental gradient and vertical niche stratification. Most Marmotini are semi-fossorial and rely on the lack of large roots in open environments to dig burrows for their nests. The Tamiini are terrestrial squirrels, with no arboreal or semi-fossorial adaptations, relying on groundcover to provide nesting sites and shelter from predators. In contrast, arboreal sciurid ecologies, utilized by the Pteromyini, rely on trees for both room and board, eating tree products and making their nests within branches high above the ground. Terrestrial and arboreal niches are easily found within a forest with shrubs or herbaceous groundcover, creating vertical layering of niches. Horizontal environmental grading could represent marginal forest environments where open grassland vegetation transitions into mixed shrubs and trees.

The range of intratribal tooth dimensions also suggests niche partitioning. Dental measurements, such as first molar area, tooth row length, and tooth row area, have been related to body mass in extant organisms, allowing for the reconstruction of body mass in extinct organisms (Hopkins, 2008). Each sciurid tribe found at Cave Basin has more than one genus present and the genera within each tribe differ in size (see appendix). This translates to a corresponding difference in body size within the taxa of each tribe. Body size is related to ecological structuring and resource division (Basset, 1995 and Wilson, 1975). We can hypothesize that these differently-sized squirrel taxa filled niches that are affected by both body size and evolutionary and ecological history (indicated by their tribal association).

Spatial and Temporal Averaging at Cave Basin

The occurrence of open, mixed, and closed habitat squirrels could be a result of biological or taphonomic spatial averaging. Biological averaging could occur if squirrels typical of one habitat had large enough home ranges, permissible enough ecologies, and the physical ability to at least travel into other habitats. However, body size influences home range and dispersal range sizes, meaning the small size of sciurids compared to ungulate taxa indicates sciurids will have comparatively small home ranges and proportionately small spatial averaging abilities (Bowman, 2002). The sciurids of Cave Basin are unlikely to be traveling far enough to spatially average the environmental signal their fossils give.

Biological averaging could also occur through prey accumulation under or at predator accumulation sites. However, both fossil material type and lack of taphonomic signature suggest this accumulation method is not responsible for the Cave Basin assemblage. The Cave Basin site has not produced sciurid post-crania. From a predation taphonomy standpoint, this would be unlikely given that dental material has been found to be proportionally more affected by digestion in both modern mammalian and avian carnivores (such as the lynx and Golden Eagle, respectively) (Hockett, 1996 and Lloveras *et al.*, 2008). In this scenario, the high rate of dental digestion compared to bone digestion should increase the proportion of bones in a sample because the weakening of the tooth’s enamel and dentine should make them more susceptible to post-digestion taphonomic destruction. However, no sciurid bones were isolated during screening, even though the bones of other non-sciurid micromammals were recovered. Additionally, both avian and carnivoran digestion have prominent effects on the appearance of teeth (Lloveras *et al.*, 2008 and Fernandez-Jalvo and Andrews, 1992). There is no indication of early or late digestion-related wear on the Cave Basin Sciuridae teeth. The most common taphonomic destruction of the Cave Basin squirrel teeth is unworn breakage on tooth margins (see fig. 4H for example), followed by presumably *in-situ* fracturing and cementation (see fig. 5b for example). Neither of these taphonomic presentations indicates predation. Given the lack of predation taphonomy we would expect if the Cave Basin Sciuridae were accumulated by predators, it seems unlikely this would be prey accumulation.

Given sedimentology patterns, widespread taphonomy-related spatial averaging is unlikely within the Cave Basin site and the greater South Fork of the Crooked River. Terrestrial paleosols deposits, not fluvial sediments, produce most of the fossil material at Cave Basin. Additionally, the fossils do not display fluvial transport weathering (pers. comm., Win McLaughlin). This suggests the Cave Basin fossils were not transported far or at all and represent a sample of the local fauna.

Temporal averaging is unlikely to have occurred as well. The boundaries between the John Day Formation, the Columbia River Basalts, the Mascall Formation, and the Rattlesnake Formation are easy to identify in Crooked River sections exposing the contacts. Temporal averaging between formations would show less distinct boundaries between the lithic units here. The sediments at Cave Basin were also deposited in paleosols (pers. comm., Win McLaughlin). These sediments were accumulating and incorporating biological material but were not disturbed (which fluvial transport and sediments might indicate). Cave Basin sediments also accumulated quickly, possibly during a period as short as half a million years (pers. comm., Ray Weldon). Processes of temporal averaging within the Cave Basin sediments would have to disturb a great volume of sediment very quickly. As there is no evidence of such an event, temporal averaging seems unlikely to have occurred at Cave Basin.

CONCLUSIONS

The sciurid assemblage at Cave Basin is one of the most diverse in Oregon. The diagnoses of the Cave Basin sciurids have important implications for squirrel taxonomy, biogeography, and ecology. The discovery of a complete (although disarticulated) dentition of *Protospermophilus oregonensis* permits the amendment of the *Protospermophilus* diagnosis and increases the variation known within the genus' dentition. The presence of *Miospermophilus paulinaensis* (Marmotini) and *cf. Miopetaurista* (Pteromyini) are both biogeographically and chronologically interesting, yet consistent with prior occurrences of the genera. *Miospermophilus* species are present in many western North America assemblages from the Arikareean to the Clarendonian. However, there were no *Miospermophilus* species known from Oregon as would be expected from general geographic distributions. *M. paulinaensis* extends the geographic range of the genus to the Pacific Northwest.

The presence of *cf. Miopetaurista* at Cave Basin is one piece of the biogeographic puzzle of flying squirrel distribution. *Miopetaurista* is well known from the Miocene of Europe and Asia, but before this study, only known in North America from the Pliocene of Florida. If the North American and Eurasian representatives are, in fact, related, we would hypothesize other representatives would be found within other North American sediments of Miocene age between Florida and the Bering Strait. The presence of *cf. Miopetaurista* in the Middle Miocene of Oregon is in line with the hypothesis of an East-from-Asia migration. Further work will help determine the timing and directionality of the migration of large Pteromyini like *Miopetaurista.* This work emphasizes the difficulties of identifying large Pteromyini in the fossil record and provides several key differences to aid in the identification of *Miopetaurista*.

Within each tribe present at Cave Basin, two or more genera of sciurids were identified. If tribal affiliations impact sciurid ecology as it does in modern squirrels, the presence of multiple genera in each tribe suggests niche partitioning. Differences in tooth size between sciurids of similar ecologies suggest body size was a factor in niche determination. The proximity of both forested, intermediate, and non-forest environments is reinforced by the indication of so many different ecologies and niches in one fauna.

The environments of Cave Basin are as diverse as the squirrels inhabiting them. The Mascall Formation material form Cave Basin provides a new window into the Mid-Miocene climatic maximum. Both sedimentological and paleontological data indicate the basin hosted intermittent lacustrine and forest margin environments, contrasting with the forests, woodland clearings, and cypress swamps of the John Day Basin Mascall formation’s alluvial floodplains. Both the John Day Basin and Cave Basin Mascall deposits indicate comparatively more forested environments than seen in both older and younger formations, which is expected in the warmer, wetter climate of the MMCO.

APPENDIX 1. DENTAL MEASUREMENTS

Taxon	Locality	Specimen	Anteroposterior Length	Transverse Length
cf. Miopetaurista	UO 4343 Cave Basin	F-69068	4.02	3.51
cf. Miopetaurista	UO 4343 Cave Basin	F-69117	3.17	3.71
cf. Miopetaurista	UO 4343 Cave Basin	F-69119	3.50	N/A
cf. Miopetaurista	UO 4343 Cave Basin	F-69120	N/A	4.38
Blackia	UO 4343 Cave Basin	F-69118	1.75	1.71
Blackia	UO 4343 Cave Basin	F-69123	1.65	1.42
Miospermophilus paulinaensis	UO 4343 Cave Basin	F-64901	1.56	1.92
Miospermophilus paulinaensis	UO 4343 Cave Basin	F-64903	N/A	1.95
Miospermophilus paulinaensis	UO 4343 Cave Basin	F-64906	1.46	1.85
Miospermophilus paulinaensis	UO 4343 Cave Basin	F-64907	1.75	2.18
Miospermophilus paulinaensis	UO 4343 Cave Basin	F-64908	2.00	1.84
Miospermophilus paulinaensis	UO 4343 Cave Basin	F-64909	1.60	1.29
Miospermophilus paulinaensis	UO 4343 Cave Basin	F-64911	1.80	1.80
Miospermophilus paulinaensis	UO 4343 Cave Basin	F-64913	1.30	N/A
Miospermophilus paulinaensis	UO 4343 Cave Basin	F-64914	1.58	1.36
Miospermophilus paulinaensis	UO 4343 Cave Basin	F-64919	1.92	1.76
Miospermophilus paulinaensis	UO 4343 Cave Basin	F-64924	2.11	2.27
Miospermophilus paulinaensis	UO 4343 Cave Basin	F-64929	1.68	2.00
Miospermophilus paulinaensis	UO 4343 Cave Basin	F-64936	1.95	2.12
Miospermophilus paulinaensis	UO 4343 Cave Basin	F-64937	1.68	1.22
Miospermophilus paulinaensis	UO 4343 Cave Basin	F-64943	1.52	1.78
Miospermophilus paulinaensis	UO 4343 Cave Basin	F-64945	1.78	2.14
Miospermophilus paulinaensis	UO 4343 Cave Basin	F-64948	1.72	2.09
Miospermophilus paulinaensis	UO 4343 Cave Basin	F-64950	1.67	1.78
Miospermophilus paulinaensis	UO 4343 Cave Basin	F-64952	1.80	2.20

Taxon	Locality	Specimen	Anteroposterior Length	Transverse Length
Miospermophilus paulinaensis	UO 4343 Cave Basin	F-64954	1.81	1.89
Miospermophilus paulinaensis	UO 4343 Cave Basin	F-64955	2.16	1.88
Miospermophilus paulinaensis	UO 4343 Cave Basin	F-64958	1.88	1.75
Miospermophilus paulinaensis	UO 4343 Cave Basin	F-64959	1.46	1.59
Miospermophilus paulinaensis	UO 4343 Cave Basin	F-64960	2.31	1.94
Miospermophilus paulinaensis	UO 4343 Cave Basin	F-64961	2.12	2.04
Miospermophilus paulinaensis	UO 4343 Cave Basin	F-69075	1.56	1.83
Miospermophilus paulinaensis	UO 4343 Cave Basin	F-69081	1.88	1.93
Miospermophilus paulinaensis	UO 4343 Cave Basin	F-69083	2.13	2.15
Miospermophilus paulinaensis	UO 4343 Cave Basin	F-69094	1.70	2.15
Miospermophilus paulinaensis	UO 4343 Cave Basin	F-69095	1.65	1.91
Miospermophilus paulinaensis	UO 4343 Cave Basin	F-69103	1.61	1.29
Miospermophilus paulinaensis	UO 4343 Cave Basin	F-69104	1.86	2.11
Miospermophilus paulinaensis	UO 4343 Cave Basin	F-69108	2.06	2.00
Miospermophilus paulinaensis	UO 4343 Cave Basin	F-69115	1.70	1.70
Miospermophilus paulinaensis	UO 4343 Cave Basin	F-69124	1.40	1.83
Miospermophilus paulinaensis	UO 4343 Cave Basin	F-69127	2.11	1.71
Nototamias	UO 4343 Cave Basin	F-69121	1.01	0.88
Petauristodon	UO 4343 Cave Basin	F-64923	1.90	2.34
Petauristodon	UO 4343 Cave Basin	F-69027	2.57	2.16
Petauristodon	UO 4343 Cave Basin	F-69109	2.58	1.95
Protospermophilus oregonensis	UO 4343 Cave Basin	F-64965	2.58	2.07
Protospermophilus oregonensis	UO 4343 Cave Basin	F-64966	2.49	2.10
Protospermophilus oregonensis	UO 4343 Cave Basin	F-64967	2.72	3.34
Protospermophilus oregonensis	UO 4343 Cave Basin	F-64969	2.62	3.50
Protospermophilus oregonensis	UO 4343 Cave Basin	F-64970	3.07	2.73

Taxon	Locality	Specimen	Anteroposterior Length	Transverse Length
Protospermophilus oregonensis	UO 4343 Cave Basin	F-64971	2.21	1.97
Protospermophilus oregonensis	UO 4343 Cave Basin	F-64972	2.55	3.42
Protospermophilus oregonensis	UO 4343 Cave Basin	F-64973	2.23	2.84
Protospermophilus oregonensis	UO 4343 Cave Basin	F-64975	2.74	2.40
Protospermophilus oregonensis	UO 4343 Cave Basin	F-64976	2.51	3.17
Protospermophilus oregonensis	UO 4343 Cave Basin	F-64977	2.79	2.30
Protospermophilus oregonensis	UO 4343 Cave Basin	F-64978	2.94	3.34
Protospermophilus oregonensis	UO 4343 Cave Basin	F-64980	2.82	3.42
Protospermophilus oregonensis	UO 4343 Cave Basin	F-64981	2.32	3.00
Protospermophilus oregonensis	UO 4343 Cave Basin	F-64983	2.74	3.10
Protospermophilus oregonensis	UO 4343 Cave Basin	F-64986	2.30	3.27
Protospermophilus oregonensis	UO 4343 Cave Basin	F-64987	2.15	3.02
Protospermophilus oregonensis	UO 4343 Cave Basin	F-64988	3.23	2.76
Protospermophilus oregonensis	UO 4343 Cave Basin	F-64989	3.32	3.02
Protospermophilus oregonensis	UO 4343 Cave Basin	F-64990	2.73	2.16
Protospermophilus oregonensis	UO 4343 Cave Basin	F-64991	2.80	2.88
Protospermophilus oregonensis	UO 4343 Cave Basin	F-64994	2.89	3.00
Protospermophilus oregonensis	UO 4343 Cave Basin	F-64997	2.85	2.99
Protospermophilus oregonensis	UO 4343 Cave Basin	F-64998	2.57	2.12
Protospermophilus oregonensis	UO 4343 Cave Basin	F-69017	2.04	2.80
Protospermophilus oregonensis	UO 4343 Cave Basin	F-69019	2.90	3.15
Protospermophilus oregonensis	UO 4343 Cave Basin	F-69021	3.00	3.04
Protospermophilus oregonensis	UO 4343 Cave Basin	F-69022	2.92	2.93
Protospermophilus oregonensis	UO 4343 Cave Basin	F-69023	2.82	2.83
Protospermophilus oregonensis	UO 4343 Cave Basin	F-69024	2.86	3.47
Protospermophilus oregonensis	UO 4343 Cave Basin	F-69025	N/A	3.34

Taxon	Locality	Specimen	Anteroposterior Length	Transverse Length
Protospermophilus oregonensis	UO 4343 Cave Basin	F-69026	2.56	3.25
Protospermophilus oregonensis	UO 4343 Cave Basin	F-69028	2.93	3.07
Protospermophilus oregonensis	UO 4343 Cave Basin	F-69029	2.92	3.36
Protospermophilus oregonensis	UO 4343 Cave Basin	F-69030	N/A	2.80
Protospermophilus oregonensis	UO 4343 Cave Basin	F-69031	2.13	2.93
Protospermophilus oregonensis	UO 4343 Cave Basin	F-69033	2.88	3.39
Protospermophilus oregonensis	UO 4343 Cave Basin	F-69035	N/A	2.83
Protospermophilus oregonensis	UO 4343 Cave Basin	F-69036	2.51	3.27
Protospermophilus oregonensis	UO 4343 Cave Basin	F-69040	2.85	3.22
Protospermophilus oregonensis	UO 4343 Cave Basin	F-69041	2.80	3.51
Protospermophilus oregonensis	UO 4343 Cave Basin	F-69043	2.43	3.13
Protospermophilus oregonensis	UO 4343 Cave Basin	F-69046	2.65	3.05
Protospermophilus oregonensis	UO 4343 Cave Basin	F-69047	2.77	3.71
Protospermophilus oregonensis	UO 4343 Cave Basin	F-69049	2.91	2.40
Protospermophilus oregonensis	UO 4343 Cave Basin	F-69050	2.73	3.13
Protospermophilus oregonensis	UO 4343 Cave Basin	F-69051	2.84	3.09
Protospermophilus oregonensis	UO 4343 Cave Basin	F-69052	2.36	3.05
Protospermophilus oregonensis	UO 4343 Cave Basin	F-69053	2.49	1.97
Protospermophilus oregonensis	UO 4343 Cave Basin	F-69054	2.61	2.96
Protospermophilus oregonensis	UO 4343 Cave Basin	F-69056	2.86	3.30
Protospermophilus oregonensis	UO 4343 Cave Basin	F-69057	2.70	2.33
Protospermophilus oregonensis	UO 4343 Cave Basin	F-69058	N/A	3.24
Protospermophilus oregonensis	UO 4343 Cave Basin	F-69059	2.51	1.99
Protospermophilus oregonensis	UO 4343 Cave Basin	F-69060	2.22	3.02
Protospermophilus oregonensis	UO 4343 Cave Basin	F-69061	2.77	3.28
Protospermophilus oregonensis	UO 4343 Cave Basin	F-69062	2.90	2.29

Taxon	Locality	Specimen	Anteroposterior Length	Transverse Length
Protospermophilus oregonensis	UO 4343 Cave Basin	F-69064	2.58	1.99
Protospermophilus oregonensis	UO 4343 Cave Basin	F-69066	2.65	3.36
Protospermophilus oregonensis	UO 4343 Cave Basin	F-69067	2.91	3.08
Protospermophilus oregonensis	UO 4343 Cave Basin	F-69079	2.57	2.02
Protospermophilus oregonensis	UO 4343 Cave Basin	F-69085	2.57	2.00
Protospermophilus oregonensis	UO 4343 Cave Basin	F-69116	3.06	2.94
Protospermophilus oregonensis	UO 4343 Cave Basin	F-69138	2.67	2.12
Protospermophilus oregonensis	UO 4343 Cave Basin	F-69139	2.66	3.48
Protospermophilus oregonensis	UO 4343 Cave Basin	F-69140	2.23	2.78
Protospermophilus oregonensis	UO 4343 Cave Basin	F-69141	2.86	3.19
Protospermophilus oregonensis	UO 4343 Cave Basin	F-69142	2.68	3.23
Protospermophilus oregonensis	UO 4343 Cave Basin	F-69143	2.92	2.99
Protospermophilus oregonensis	UO 4343 Cave Basin	F-69145	2.78	2.24
Protospermophilus oregonensis	UO 4343 Cave Basin	F-69146	2.43	3.39
Protospermophilus oregonensis	UO 4343 Cave Basin	F-69147	2.08	2.96
Protospermophilus oregonensis	UO 4343 Cave Basin	F-69148	2.64	3.11
Protospermophilus oregonensis	UO 4343 Cave Basin	F-69149	2.69	3.32
Protospermophilus oregonensis	UO 4343 Cave Basin	F-69151	2.92	3.35
Protospermophilus oregonensis	UO 4343 Cave Basin	F-69152	2.65	2.88
Protospermophilus oregonensis	UO 4343 Cave Basin	F-69153	3.03	2.82
Protospermophilus oregonensis	UO 4343 Cave Basin	F-69154	N/A	3.32
Protospermophilus oregonensis	UO 4343 Cave Basin	F-69156	2.75	3.16
Protospermophilus oregonensis	UO 4343 Cave Basin	F-69157	2.84	2.85
Protospermophilus oregonensis	UO 4343 Cave Basin	F-69158	2.73	3.46
Protospermophilus oregonensis	UO 4343 Cave Basin	F-69160	2.96	3.28
Protospermophilus oregonensis	UO 4343 Cave Basin	F-69161	2.69	3.07

Taxon	Locality	Specimen	Anteroposterior Length	Transverse Length
Protospermophilus oregonensis	UO 4343 Cave Basin	F-69163	3.03	3.19
Protospermophilus oregonensis	UO 4343 Cave Basin	F-69164	N/A	3.18
Protospermophilus oregonensis	UO 4343 Cave Basin	F-69168	2.76	2.94
Protospermophilus oregonensis	UO 4343 Cave Basin	F-69170	2.97	3.10
Protospermophilus oregonensis	UO 4343 Cave Basin	F-69172	2.65	2.59
Protospermophilus oregonensis	UO 4343 Cave Basin	F-69173	2.85	2.43
Protospermophilus oregonensis	UO 4343 Cave Basin	F-69176	2.70	3.23
Protospermophilus oregonensis	UO 4343 Cave Basin	F-69177	2.65	2.08
Protospermophilus oregonensis	UO 4343 Cave Basin	F-69178	2.94	3.47
Protospermophilus oregonensis	UO 4343 Cave Basin	F-69181	2.85	2.80
Protospermophilus oregonensis	UO 4343 Cave Basin	F-69182	2.77	2.92
Protospermophilus oregonensis	UO 4343 Cave Basin	F-69183	N/A	2.56
Protospermophilus oregonensis	UO 4343 Cave Basin	F-69184	2.64	2.78
Protospermophilus oregonensis	UO 4343 Cave Basin	F-69185	2.62	N/A
Protospermophilus oregonensis	UO 4343 Cave Basin	F-69186	2.39	3.08
Protospermophilus oregonensis	UO 4343 Cave Basin	F-69187	2.81	3.01
Protospermophilus oregonensis	UO 4343 Cave Basin	F-69188	2.61	3.37
Protospermophilus oregonensis	UO 4343 Cave Basin	F-69189	2.60	3.29
Protospermophilus oregonensis	UO 4343 Cave Basin	F-69192	2.56	3.21
Protospermophilus oregonensis	UO 4343 Cave Basin	F-69193	2.64	3.36
Protospermophilus oregonensis	UO 4343 Cave Basin	F-69194	2.60	2.20
Protospermophilus oregonensis	UO 4343 Cave Basin	F-69195	2.55	3.09
Protospermophilus oregonensis	UO 4343 Cave Basin	F-69196	2.98	3.27
Protospermophilus oregonensis	UO 4343 Cave Basin	F-69197	2.22	3.00
Protospermophilus oregonensis	UO 4343 Cave Basin	F-69198	2.57	3.17
Protospermophilus oregonensis	UO 4343 Cave Basin	F-69200	2.99	3.25

Taxon	Locality	Specimen	Anteroposterior Length	Transverse Length
Protospermophilus oregonensis	UO 4343 Cave Basin	F-69204	3.11	N/A
Protospermophilus oregonensis	UO 4343 Cave Basin	F-69205	2.78	3.48
Protospermophilus oregonensis	UO 4343 Cave Basin	F-69206	2.44	3.06
Protospermophilus oregonensis	UO 4343 Cave Basin	F-69207	3.24	2.81
Protospermophilus oregonensis	UO 4343 Cave Basin	F-69208	3.25	2.85
Tamias	UO 4343 Cave Basin	F-64910	1.39	1.30
Tamias	UO 4343 Cave Basin	F-64947	1.34	1.06
Tamias	UO 4343 Cave Basin	F-69087	1.97	N/A
Tamias	UO 4343 Cave Basin	F-69130	1.65	1.35
Tamias	UO 4343 Cave Basin	F-69133	1.33	1.01
Tamias	UO 4343 Cave Basin	F-69134	1.55	1.76
Tamias	UO 4343 Cave Basin	F-69135	1.46	1.07

N/A indicates the tooth was broken or damaged, preventing the measuring of its length.

APPENDIX 2. SELECTED GLOSSARY

Arboreal	Describing a tree-dwelling lifestyle
Benthic	Describing the deepest depths in a body of water
Biogeography	The patterns of animals’ distributions across the earth
Biostratigraphy	The order of fossils within and between layers of sediment relating to the age of the fossil
Community	A group of organisms living in a specific place at a specific time
Dentition	The teeth of a taxon
Diatomite	A rock formed through the accumulation of diatoms (algae with silicon cell walls) living and dying in a body of water
Dispersal range	The distance an animal can migrate over its lifetime that is outside its normal travels *e.g.* the immigration of individuals
Fauna(l)	Of, relating to, or belonging to Animalia
Flora(l)	Of, relating to, or belonging to Plantae
Fluvial	Of or relating to a river
Fossorial	Describing an underground or burrowing lifestyle
Home range	The distance an animal regularly travels during its regular activities *e.g.* finding resources
Lacustrine	Of or relating to a lake
Macrofauna(l)	Large animals *e.g.* a horse
Macroflora(l)	Plant material that can be easily seen with the naked eye *e.g.* a leaf
Matrix	The material surrounding an object of interest *e.g.* sediment around a fossil
Microfauna(l)	Small animals *e.g.* a squirrel

Microflora(l)	Microscopic plant material *e.g.* pollen or individual alga
Niche	The role or combination of roles taken by an organism in a community
Paleoecology	The study of ancient ecosystems through the fossilized remains of the fossilized plants, animals, and soils
Paleopedology	The study of fossilized soils
Paleosol	A ‘fossil’ soil
Palynology	The study of fossilized pollen
Phytolith(s)	A microscopic mineral fragment formed within plant tissues
Sciuridae	The squirrel family
Sediment	Fragmented solid material deposited in layers on the earth’s surface by biological and non-biological processes
Spatial averaging	A process where (fossiliferous) material from near and distant places mix, reflecting an average of the individual places the material originated in but perhaps no specific signal
Stratigraphy	The order of layers of sediment on the earth’s surface in a particular place
Taphonomy	Any and all processes occurring to biological material after its death, including predation, wear, fossilization, and/or destruction
Temporal averaging	A process where (fossiliferous) material from a large span of time mixes, giving a temporal signal that is not reflective of one time period.
Terrestrial	Describing a ground-dwelling lifestyle
Tuff	A rock formed through the accumulation of volcanic ash

BIBLIOGRAPHY

Agadjanian, A. 2010. Development of small mammal communities in the Don River basin during the Pliocene and Pleistocene. Abstract at 2010 International Union for Quaternary Research (INQUA) Section on European Quaternary Stratigraphy (SEQS) 2010 Annual Meeting: 7.

Barlow, N. G. 1990. Application of the inner Solar System cratering record to the Earth in Global Catastrophes in Earth History: An Interdisciplinary Conference on Impacts, Volcanism, and Mass Mortality, GSA Special Paper 247: 181-187.

Basset, A. 1995. Body Size‐ Related Coexistence: An Approach Through Allometric Constraints on Home‐ Range Use. Ecology, 76(4): 1027-1035.

Bestland, E. and *et al*. 2008. Stratigraphy, paleopedology, and geochemistry o the middle Miocene Mascall Formation (type area, Central Oregon, USA). PaleoBios 28(2): 41-61.

Black, C. C. 1963. A review of the North American tertiary Sciuridae. Bulletin of the Museum of Comparative Zoology 130(3): 109-248.

Bowman, J. and *et al*. 2002. Dispersal distance of mammals is proportional to home range size. Ecology 83(7): 2049-2055.

Casanovas-Vilar, I. *et al*. 2015. Late Miocene flying squirrels from Can Llobateres 1 (Valles-Penedes Basin, Catalonia) in Systematics and Palaeobiogeography in Old worlds, new ideas: A tribute to Albert van der Meulen. Palaeobiodiversity and Palaeoenvironments 3: 20 pgs.

Chaney, R. W. 1925. The Mascall flora; its distribution and climatic relation. Carnegie Institution of Washington Publications 349: 23-48.

Chaney, R. W. 1956. The ancient forests of Oregon. Condon Lectures, Oregon State System of Higher Education, University of Oregon, Eugene, OR

Dalquest, W. W. *et al*. 1996. Fossil mammals from a late Miocene (Clarendonian) site in Beaver County Oklahoma in Contributions in Mammalogy: A memorial volume honoring Dr. J. Knox Jones, Jr. Museum of Texas Tech University: 107-137.

Daxner-Höck, G. 2004. Flying squirels (Pteromyinae, Mammalia) from the Upper Miocene of Austria. Annalen des Naturhistorischen Museums in Wien. Serie A für Mineralogie und Petrographie, Geologie und Paläontologie, Anthropologie und Prähistorie 106: 387-423.

de Bruijn, H. 1997. 6. Rodentia (Mammalia). Vertebrates from the Early Miocene lignite deposits of the opencast mine Oberdorf (Western Styrian Basin, Austria). Naturhistorisches Museum 99: 99-137

Dillhoff, R. M. and *et al*. 2009. Cenozoic paleobotany of the John Day Basin, central Oregon. The Geologic Society of America Field Guides 15.

Downing, K. F. 1992. Biostratigraphy, taphonomy, and paleoecology of vertebrates from the Sucker Creek Formation (Miocene) of Southeastern Oregon. Ph.D. dissertation, University of Arizona Tucson, Arizona: 1-485.

Downs, T. 1956. The Mascall fauna from the Miocene of Oregon. University of California Publications in Geological Science 31(5): 199-354.

Dunn, R. E. 2014. A middle Miocene phytolith record from western North America, the Mascall Formation of eastern Oregon. Abstract at Botany 2014 Annual Meeting. Boise, Idaho.

Dunn, R. E. and Stromberg, C. A. E. 2014. The vegetational context for rodent evolution in the Pacific Northwest: Middle Miocene phytoliths the Mascall Formation of Eastern Oregon. Abstract at GSA 2014 Annual Meeting. Vancouver, British Columbia.

Engesser, B. 1979. Relationships of some insectivores and rodents from the Miocene of North America and Europe. Bulletin of Carnegie Museum of Natural History 14: 1-68.

Fernandez-Jalvo and Andrews. 1992. Small Mammal Taphonomy of Gran Dolina, Atapuerca (Burgos), Spain. Journal of Archaeological Science 19: 407-428.

Gazin, C. L. 1930. A tertiary vertebrate fauna from the Upper Cuyama drainage basin, California. Carnegie Institution of Washington Publications 404: 55-76.

Gazin, C. L. 1932. A Miocene mammalian fauna from south-eastern Oregon. Carnegie Institution of Washington Publications 418: 37-86.

Goodwin, T. H. 2008. Sciuridae in Evolution of Tertiary Mammals of North America Volume 2: small mammals, xenarthrans, and marine mammals. Cambridge University Press.

Gray, J. 1960. Fossil Chlorophycean algae from the Miocene of Oregon. Journal of Paleontology 34(3): 453-463.

Hockett, B. S. 1996. Corroded, Thinned and Polished Bones Created by Golden Eagles (*Aquila chrysaetos*): Taphonomic Implications for Archaeological Interpretations. Journal of Archaeological Science 23: 587–591.

Hopkins, S.S. 2008. Reassessing the mass of exceptionally large rodents using toothrow length and area as proxies for body mass. Journal of Mammalogy, 89(1): 232-243.

James, G. T. 1963. Paleontology and non-marine stratigraphy of the Cuyama Valley Badlands, California: Part 1. Geology, faunal interpretations, and systematic description of Chiroptera, Insectivora, and Rodentia. University of California Publications in Geological Science 45: 1-171.

Kelt, D. A. and D. Van Vuren. 1999. Energetic constraints and the relationship between body size and home range area in mammals. Ecology 80(1): 337-340.

Kerbis Peterhans, J. C. *et al*. 1993. A contribution to tropical rain forest taphonomy: retrieval and documentation of chimpanzee remains from Kibale Forest, Uganda. Journal of Human Evolution 25(6): 485-514.

Kohn, M. J. and T. J. Fremd. 2008. Miocene tectonics and climate forcing of biodiversity, western United States. Geology 36(10): 783-786.

Korth, W. W. 1992. Small mammals from the Harrison Formation (late Arikareean, early Miocene), Cherry County, Nebraska. Annals of Carnegie Museum 61(2): 69-131.

Li, C. and *et al*. 1983. The Aragonian vertebrate fauna of Xiacaowan, Jiangsu. Vertebrata Palasiatica 21(4): 313-327.

Lindsay, E. H. 1971. Small mammal fossils from the Barstow Formation, California. University of California Publications in Geological Science 93: 1-104.

Lloveras *et al.* 2008. Taphonomic analysis of leporid remains obtained from Modern Iberian Lynx (Lynx pardinus) scats. Journal of Archaeological Science 35: 1-13.

Lu, X. and *et al*. 2013. The evolution and paleobiogeography of flying squirrels (Sciuridae, Pteromyini) in response to global environmental change. Evolutionary Biology 40: 117-132.

Maguire, K. C. 2015. Dietary niche stability of equids across the mid-Miocene climatic optimum in Oregon, USA. Palaeogeography, Palaeoclimatology, Palaeoecology 426: 297-307.

McCarty, R. and Congleton, J. 1994. Heavy liquids: Their use and methods in paleontology. Vertebrate paleontological Techniques Volume One: 187- 204.

McLaughlin, W. F. *et al*. 2016. A new Late Hemingfordian vertebrate fauna from Hawk Rim, Oregon, with implications for biostratigraphy and geochronology. Journal of Vertebrate Paleontology.

Mein, P. 1970. Les Sciuropteres (Mammalia, Rodentia) Neogenes d'Europe occidentale. GeoBios 3(3): 7-77.

Oshida, T. *et al*. 2000. Phylogenetic relationships among six flying squirrel genera inferred from mitochondrial cytochrome b gene sequences. Zoological Science 17(4): 485-489.

Pratt, A. E. and G. S. Morgan. 1989. New Sciuridae (Mammalia: Rodentia) from the early Miocene Thomas Farm Local Fauna, Florida. Journal of Vertebrate Paleontology 9(1): 89-100.

Qiu, Z. and C. Li. Rodents from the Chinese Neogene: Biogeographic Relationships with Europe and North America. Vertebrate fossils and their context: contributions in honor of Richard H. Tedford. Bulletin of the American Museum of Natural History 279: 586-602.

Qui, Z. 2002. Sciurids from the Late Miocene Lufeng hominid locality, Yunnan. Vertebrata Palasiatica 40(3): 177-193.

Rasband, W.S. 1997-2016. ImageJ. U. S. National Institutes of Health, Bethesda, Maryland, USA, http://imagej.nih.gov/ij/.

Retallack, G. J. 2009. Cenozoic cooling and grassland expansion in Oregon and Washington. PaleoBios 28(3): 89-113.

Robertson, J. S. Jr. 1970. Blancan mammals from Haile XVA, Alachua County, Florida. Ph.D. Dissertation, University of Florida, Gainesville, Florida, 172 pp.

Sheldon, N. D 2006. Using paleosols of the Picture Gorge Basalt to reconstruct the middle Miocene climatic optimum. PaleoBios 26(2): 27-36.

Shevyreva, N. S. and G. I. Baranova. 2003. Sciuromorpha (Rodentia) from the Miocene of Zaissan Depression, Eastern Kazakhstan. Russian Journal of Theriology 2(1): 9-13.

Shotwell, J. A. 1968. Miocene mammals of Southeast Oregon. Bulletin of the Museum of Natural History, University of Oregon 14: 1-67.

Skwara, T. 1986. A new "flying squirrel" (Rodentia: Sciuridae) from the early Miocene of Southwestern Saskatchewan. Journal of Vertebrate Paleontology 6(3): 290-294.

Soil Survey Staff. 1999. Soil Taxonomy, Second Edition, Agriculture Handbook Number 436. United States Department of Agriculture- Natural Resources Conservation Service.

Steppan, S. J. *et al*. 2004. Nuclear DNA phylogeny of the squirrels (Mammalia: Rodentia) and the evolution of arboreality from c-myc and RAG1. Molecular phylogenetics and evolution 30: 703-719.

Streck, M. J. and A. L. Grunder. 1995. Crystallization and welding variations in a widespread ignimbrite sheet; the Rattlesnake tuff, eastern Oregon, USA. Bulletin of Volcanology 57: 151-169.

Tappen, M. 1994. Bone weathering in the tropical rain forest. Journal of Archeological Science 21(5): 667-673.

Wallace, R. E. 1946. A Miocene mammalian fauna from Beatty Buttes, Oregon. Contributions to Paleontology: 114-134.

Webb, S. D. *et al*. Terrestrial mammals of the Palmetto Fauna (early Pliocene, latest Hemphillian) from the Central Florida Phosphate District. Geology and Vertebrate Paleontology of Western and Southern North America: Contributions in Honor of David P. Whistler. Natural History Museum of Los Angeles County Science Series 41: 293-312.

Wilson, D.S. 1975. The adequacy of body size as a niche difference. The American Naturalist, 109(970): 769-784.